RNAi-based screen for cuticle pigmentation in *Drosophila melanogaster* reveals novel regulators of brain dopamine

Samantha L Deal[1,2], Danqing Bei[2,3], Shelley B Gibson[2,3], Harim Delgado-Seo[2,4], Yoko Fujita[2,3], Kyla Wilwayco[2,3], Elaine S Seto[5,6,7], Shinya Yamamoto[1,2,3,4,8,#]

[1] Program in Developmental Biology, Baylor College of Medicine (BCM), Houston, TX 77030, USA

[2] Jan and Dan Duncan Neurological Research Institute (NRI), Texas Children's Hospital (TCH), Houston, TX 77030, USA

[3] Department of Molecular and Human Genetics, BCM, Houston, TX 77030, USA

[4] Department of Neuroscience, BCM, Houston, TX 77030 USA

[5] Department of Neurology, TCH, Houston, TX 77030, USA

[6] Epilepsy Center, TCH, Houston, TX 77030, USA

[7] Department of Neurophysiology, TCH, Houston, TX 77030, USA

[8] Development, Disease Models & Therapeutics Graduate Program, BCM, Houston, TX 77030, USA

#Corresponding Author: Shinya Yamamoto

E-mail: yamamoto@bcm.edu; Phone: 832-824-8119; Fax: N/A

Keywords: *Drosophila melanogaster*, dopamine, pigmentation, RNAi, screen, *clueless*, *mask*

Abstract

The dopaminergic system has been extensively studied for its role in behavior in various animals as well as human neuropsychiatric and neurological diseases. However, we still know little about how dopamine levels are tightly regulated *in vivo*. In order to identify novel regulators of dopamine levels, we utilized *Drosophila melanogaster* cuticle pigmentation as a readout, where dopamine is used as a precursor to melanin. First, we measured dopamine from classical mutants of genes that are known to be important for cuticle pigmentation to understand the relationship between dopamine levels and cuticle color. We then performed an RNAi-based screen to identify novel regulators of cuticle pigmentation. We identified 153 genes that were not only enriched for conserved homologs and disease-associated genes, but were unexpectedly enriched for multiple developmental signaling pathways and mitochondria-associated proteins. Upon measuring dopamine from 35 prioritized candidates from this cohort, we found 10 that caused significant reduction in dopamine in the head while one caused an increase. While most of these 11 genes are expressed in the fly brain, only two of them, *clu* and *mask,* altered dopamine levels specifically in the brain upon knockdown in dopaminergic cells. Interestingly, *mask* may act as a hub of dopamine regulation since it is associated with three nodes found in our screen (Receptor tyrosine kinase/EGF signaling, Hippo signaling, and mitochondrial dynamics). Further examination suggests that Mask likely acts on dopamine synthesis by regulating transcription of the rate-limiting dopamine synthesis enzyme, *tyrosine hydroxylase*. In conclusion, this screen identified 11 new regulators of dopamine levels and provides molecular handles to investigate how dopamine levels are controlled *in vivo*, as well as revealed an unexpected relationship between fly pigmentation genes, developmental signaling and human neurological and neurodevelopmental disease genes.

43 # Introduction

44 Dopamine is a conserved neurotransmitter that functions in the nervous system to regulate
45 variety of behaviors, including learning & memory, locomotion, reward, and sleep. In humans,
46 disruptions in dopamine have been associated with neurological and neuropsychiatric disorders,
47 including addiction, depression, sleep disorders, and schizophrenia (Grace 2016; Nutt et al. 2015;
48 Radwan et al. 2019). In addition, one of the hallmarks of Parkinson's disease is early degeneration
49 of dopaminergic neurons, and Parkinson's patients are often given a dopamine precursor, l-
50 dihydroxyphenylalanine (L-DOPA), as a method for treating symptoms (Church 2021; Armstrong
51 and Okun 2020). Most genetic research on dopamine biology has focused on dopaminergic
52 signaling and transport; however, changes in dopamine levels can have a great impact on
53 behavioral outcomes (López-Cruz et al. 2018; Steiner and Kitai 2001; Rohwedder et al. 2016).
54 Thus, identifying genes that affect dopamine levels is critical to understanding and potentially
55 treating dopamine-associated disorders.

56 Dopamine synthesis is a conserved process, whereby the amino acid tyrosine gets
57 converted into L-DOPA via the rate-limiting enzyme, Tyrosine hydroxylase (TH) (Budnik and
58 White 1987). Then, L-DOPA is converted into dopamine via the enzyme Dopa decarboxylase
59 (Ddc) (Livingstone and Tempel 1983), which is also an important enzyme for the biosynthesis of
60 serotonin. In mammals, dopamine can be degraded either via oxidation or methylation using the
61 enzymes Monoamine oxidase (MAO) and Catechol-O-methyltransferase (COMT), respectively
62 (Meiser et al., 2013). In invertebrates, the primary methods for dopamine degradation are thought
63 to be β-alanylation via the β-alanyl amine synthase (encoded by the *ebony* gene in *Drosophila*
64 *melanogaster*), and acetylation via the acetyltransferase (encoded by the *speck* gene in
65 *Drosophila*) (Yamamoto and Seto 2014). However, insects also convert dopamine into melanin
66 to form the proper cuticle pigment and structure. In fact, changes in genes that are involved in
67 dopamine metabolism lead to changes in cuticle color (Spana et al. 2020; True et al. 1999;

68 Wittkopp et al. 2002). In other words, knockdown of *TH* (known as the *pale (ple)* gene in
69 *Drosophila*) or *Ddc* leads to a paler cuticle, and mutations or knockdown of *ebony* or *speck* leads
70 to a darker cuticle.

71 Historically, *Drosophila* has been used to study dopamine biology in multiple contexts.
72 Early establishment of behavioral assays in the fly identified that the dopaminergic neurons
73 (DANs) that innervate the mushroom body are critical for learning and memory (Gervasi et al.
74 2010; Heisenberg et al. 1985). Over the years, an extensive genetic toolkit has been generated
75 in the fruit fly, making it a great system for dissecting dopaminergic neural circuitry and signaling
76 involved in many behavioral contexts (Jenett et al. 2012; Frighetto et al. 2022; Xie et al. 2018). In
77 addition to the fly's contribution to understanding dopaminergic circuitry, this model organism has
78 also been used to identify and investigate the cellular functions of Parkinson disease's genetic
79 risk factors such as *PINK1* and *PRKN* (i.e. *Pink1* and *parkin* in the fruit fly, Clark et al. 2006). The
80 conservation of systems and mechanisms in neural biology along with the efficiency of working in
81 *Drosophila* has made it a great system for large-scale screening of novel genes involved in a
82 phenotype of interest. Previously, a large-scale RNAi screen (11,619 genes, ~89% of genome)
83 was performed to identify genes that affect mechanosensory organs and cuticle formation in the
84 *Drosophila* thorax (Mummery-Widmer et al. 2009). In this screen, the researchers found 458
85 genes that affected cuticle color upon knockdown, but no further validation was performed.

86 In this manuscript, we attempted to utilize the fruit fly cuticle to identify novel regulators of
87 dopamine. We started by systematically examining classical pigmentation genes for their effect
88 on dopamine in the head and brain. From this we found that genes that are involved in dopamine
89 synthesis are the only genes with expected effects on dopamine; genes involved in degradation
90 of dopamine either have no effect or unexpectedly show reduced dopamine. We next went on to
91 characterize the 458 genes identified from the RNAi screen by Mummery-Widmer et al. (2009).
92 We tested 330 of them with independent RNAi lines and found 153 genes (~46%) with consistent
93 cuticle pigmentation defects. After prioritizing these genes based on their cuticle effects, potential

links to human diseases and their roles in the brain, we examined their effects on dopamine in the head and brain. From this analysis, we found two genes, *mask* and *clu*, that upon knockdown significantly reduce dopamine in the brain, and further show that *mask* affects mRNA and protein levels of TH.

Results

Drosophila pigmentation genes affect dopamine in unexpected ways

To systematically test if changes in pigmentation genes affect dopamine as theorized in the field, we characterized loss-of-function alleles of genes involved in dopamine metabolism (Figure 1A) for pigmentation phenotypes and dopamine levels in the head and brain. The enzymes required for dopamine synthesis, TH and Ddc, are essential for survival (Pendleton et al. 2002; Wright et al. 1976). Thus, we took advantage of established RNAi lines (Ni et al. 2009; Pan et al. 2022; Riemensperger et al. 2013) and UAS/GAL4 system (Brand and Perrimon 1993) to examine their effects. It is well documented and accepted that reduction of *TH* or *Ddc* levels or activity causes pale pigmentation and reduction of dopamine levels (True et al. 1999; Livingstone and Tempel 1983; Budnik and White 1987). By knocking down *TH* using a UAS-RNAi transgene that have been previously validated using a *TH-GAL4* driver (Bayersdorfer et al. 2010), the effect of which is highlighted by the strength of the pale cuticle phenotype (Figure 1B-C), we found total head dopamine levels to be reduced by ~60% (Figure 1E) and brain dopamine levels by ~32% (Figure 1E'). On the other hand, *Ddc* knockdown causes a weaker effect than *TH* RNAi in the cuticle (Figure 1B,D) and in the head (~35% dopamine reduction, Figure 1E), and we did not observe a significant effect on dopamine in the brain (Figure 1E'). This may be due to the strength of the RNAi and/or enzyme level requirements (since TH is known to be the rate-limiting enzyme with a more restricted expression pattern).

To test the genes that have been implicated in dopamine degradation and cuticle development (pigmentation and structural rigidity), we examined mutants that are thought to be

119 null or strong hypomorphic alleles. These alleles cause darker or paler cuticle formation (Figure
120 1F-1L, 1F'-1L') depending on their role in the melanin formation. While we expected to see
121 elevated levels of dopamine or possibly no effect for most of these alleles, *black*, *speck*, *straw*
122 and *yellow* mutants caused a reduction in dopamine in the head (Figure 1Q). Mutants for *ebony*
123 and *tan* on the other hand had no significant effect on head dopamine levels (Figure 1Q). In order
124 to identify if any of these alleles are likely to affect brain dopamine levels, we first asked if any of
125 them show expression in the brain using publicly available T2A-GAL4 gene trap lines (Diao et al.
126 2015; Lee et al. 2018; Kanca et al. 2019). Based on our own expression analysis (Figure 1 M-P)
127 and previously reported expression data (Hovemann et al., 1998; Richardt et al., 2002), several
128 of these genes are expressed in the fly brain but their expression does not appear to overlap with
129 DA neurons. When we measured effects of these mutants on brain dopamine levels (Figure 1R),
130 we found that mutations in these pigmentation genes do not significantly affect brain dopamine
131 levels.

132 Together this data shows that while changes in dopamine synthesis causes a paler cuticle,
133 which reflects a reduction in dopamine in the head and brain, changes in dopamine metabolism
134 enzymes downstream of dopamine synthesis cause pigmentation phenotypes that do not
135 correlate with head or brain dopamine level differences in adulthood.

136

137 **RNAi-based cuticle pigmentation screen**

138 From mining a previously published genome-wide scale RNAi screen (Mummery-Widmer
139 et al. 2009), we identified 458 genes with pigmentation defects that were discovered using
140 *pannier(pnr)-GAL4*, which is expressed in the dorsocentral nota. In order to check if these
141 phenotypes can be reproduced using independent reagents, we located 718 additional UAS-RNAi
142 lines for 330 of these genes from alternative sources. 426 of these lines were from the National
143 Institute of Genetics in Mishima, Japan (Yamamoto-Hino et al. 2015), and 292 of them came from
144 the Transgenic RNAi Project (TRiP) at Harvard Medical School (Ni et al. 2009). Upon screening

145 these RNAi's using the same *pnr-GAL4* driver, we found that 153 genes caused pigmentation
146 defects in at least one additional RNAi line, showing a validation of 46.4% of the hits for the
147 previous screen (Figure 2A).

148 Our RNAi-based pigmentation secondary screen produced a broad spectrum of
149 phenotypes (Figure 2B). When we classified these phenotypes into three categories, mild,
150 moderate, or strong, we found that these three categories were equally represented (mild = 38%,
151 moderate = 33%, strong = 29%, Figure 2D). When we scored for pigmentation color changes, we
152 saw three primary categories, pale, dark, or mix (a combination of pale and dark in a single
153 thorax). These categories were not equally represented (Figure 2E), with dark cuticle phenotypes
154 representing the majority (56%) of genes. Pale cuticle effects were found in 28% of genes, and
155 those with a mixed phenotype only represented 16%.

156 In order to classify what categories of genes cause pigmentation effects in our cohort, we
157 performed a protein-network analysis (Figure 2C). We found a group of proteins that have been
158 previously linked to cuticle pigmentation as expected, but we also found clusters related to RNA
159 processing, ubiquitin proteasome system, mitochondria-associated proteins, and signaling
160 pathway genes, Hippo and EGF (epidermal growth factor) signaling in particular. GO enrichment
161 analysis also highlighted terms associated with cuticle pigmentation, protein stability, and several
162 signaling pathways (Supplemental Figure 1). In addition to this, we also observed that 85% of our
163 genes were conserved between *Drosophila* and human (57.9% of genes are conserved between
164 the two species (Yamamoto et al. 2023), an enrichment from the 68% of fly genes conserved in
165 genes tested the original RNAi screen (Figure 2F, Supplemental Figure 2).

166 In summary, the cuticle pigmentation screen identified a broad spectrum of pale, dark and
167 mixed phenotypes in 152 genes, showing that for cuticle color ~50% of RNAi hits can be validated.
168 Close examination of these hits highlighted that many of them are conserved and implicated in
169 unexpected molecular processes, such as developmental signaling.

170

171 **Many pigmentation genes isolated have a neurological consequence**

172 To assess if any of the genes identified as hits from our pigmentation genes have a
173 neurological consequence, and thus might cause an effect on dopamine in the brain, we checked
174 if any of the homologs have a neurological disease association. We found that 51.2% of the fly
175 genes with a human homolog are associated with some type of disease and of those disease-
176 causing genes 78% have at least one disease that leads to a neurological phenotype (Table 1,
177 Supplemental Figure 2). Among the neurological phenotypes identified, there were a broad
178 spectrum of symptoms noted, including intellectual disability, autism spectrum disorder, ataxia,
179 epilepsy, and cerebral atrophy.

180 In addition to classifying neurological consequences in homologous human genes, we
181 directly assessed neurological consequences in the fly. Since dopamine is known to regulate
182 locomotion and sleep (Riemensperger et al. 2011; Pendleton et al. 2002), we screened for
183 locomotion and sleep defects using the Drosophila Activity Monitor (DAM; Chiu et al. 2010). We
184 tested 274 RNAi lines from the NIG, TRiP, and VDRC RNAi collections (Dietzl et al. 2007; Ni et
185 al. 2011; Vissers et al. 2016) corresponding to 152 genes that showed consistent pigmentation
186 defects. These lines were driven using *TH-GAL4* and scored for changes in total locomotion, total
187 sleep, sleep bout length, and sleep latency during the night and day (Figure 3). There was a broad
188 range in the RNAi lines for each of these phenotypes (Figure 3E-H). Since we tested different
189 RNAi lines from multiple sources that were made using different techniques, we focused on RNAi
190 lines that behaved as “outliers” by identifying hits that were two standard deviations from the mean
191 for a given phenotype. Each phenotype showed a similar number of “outliers” (locomotion: 23
192 lines, total sleep: 20 lines, sleep bout length: 21 lines, sleep latency: 25 lines). While total sleep
193 and locomotion strongly overlapped with each other, sleep latency and sleep bout length did not
194 overlap very well with the other sleep phenotypes (Figure 3D). Genes that affect sleep can often
195 show distinct phenotypes that do not necessarily correspond to multiple phenotypes or times of
196 day (Shafer and Keene 2021), so any gene with one phenotype during the day or night was

197 classified as an “outlier”. Sixty lines, which corresponded to 50 genes, were classified as an
198 “outlier” for at least one phenotype.

199 Taken together, we found that 77 of our 132 conserved genes are likely to have a
200 neurological function, either because they are implicated in a human neurological disease (52
201 genes) or have been classified as behavioral “outlier” in our locomotion and sleep analysis (45
202 genes).

203

204 **Dopamine levels in the fly head were significantly altered in 11 genes**

205 To prioritize our gene list for dopamine measurement, we identified which of our genes
206 were conserved (130 conserved/152 pigmentation genes). Then, we prioritized these based on
207 whether knockdown of these genes showed a strong pigmentation effect in the cuticle (38 genes),
208 a behavioral effect in the DAM (45 genes), and/or a human neurological disease association (52
209 genes). About 72% of the genes (95/132 conserved genes) were represented in one of these
210 categories, and 29% (39/132 conserved genes) were represented in at least two (Figure 4A). We
211 classified any gene that fit into at least two of these categories as a priority hit and tested them
212 for changes in dopamine in the head using High Performance Liquid Chromatography (HPLC).
213 Using our system, we can repeat previous results that show that knocking down *TH* using an
214 RNAi or overexpressing a *TH* cDNA using *TH-GAL4* significantly reduces or increases head
215 dopamine without any effect on serotonin (Figure 4B,C, Bayersdorfer et al. 2010).

216 When we examined the 35 prioritized genes (note: some genes were not tested due to
217 lethality or stock issues), we found that 11 of them (not including *TH*) significantly alter head
218 dopamine levels (Figure 4D,E). We found that NIG lines showed about ~80% dopamine levels
219 compared to the TRiP collection (Supplemental Figure 3), so we decided to compare the DA
220 levels to neutral control lines appropriate for each collection (e.g. UAS-lacZ RNAi) to assess the
221 relative decrease or increase of dopamine. Hits from both collections show similar patterns
222 compared to the controls. First, unlike what we saw in cuticle pigmentation, where 65% of genes

223 caused a dark cuticle (excludes mixed cuticle phenotype for simplicity), most genes trended
224 toward a reduction in dopamine (71%, 25/35, Figure 4F,G). Among the 11 genes that significantly
225 alter dopamine, 10 of them (91%) significantly reduced dopamine and only one gene increased
226 dopamine. In addition, there was no direct correlation between the cuticle color and the dopamine
227 level in the fly head (Figure 4H).

228 In summary, our HPLC analysis on fly heads revealed 11 genes that significantly affect
229 dopamine levels. We saw a trend in reduction in dopamine across all lines tested as well as those
230 with significant changes, and we observed no correlation between cuticle color and dopamine
231 level, which is similar to what we observed in the classical pigmentation genes (Figure 1).

232

233 **Brain analysis reveals *mask* and *clu* as potential regulators of dopamine in the**
234 **brain**

235 To determine which of the 11 genes that affect dopamine in the head can have
236 consequences on the brain, we examined the expression of four of them in the brain using
237 available T2A-GAL4 lines (Diao et al. 2015; Lee et al. 2018; Kanca et al. 2019). We found that
238 each of these genes show some expression in the brain. Two of these genes show very broad
239 expression (*Bsg and ClC-c,* Figure 5A,B) and appear to overlap with most if not all DANs. Two
240 others showed a slightly more selective neuronal expression (*PIG-A* and *rk*, Figure 5C,D), and
241 they seem to overlap with somewhere between 30-50% of DANs. In addition, when we explored
242 publicly available single-cell mRNA sequencing datasets, ten of our gene hits (all except *Spn38F*)
243 show some expression in the brain with varying amount of overlap with TH expressing DANs
244 (Janssens et al. 2022; Li et al. 2022).

245 In order to test for changes in brain dopamine levels, we wanted to generate a line that
246 hits most if not all DANs. The *TH-GAL4* line commonly used for dopamine studies and in our
247 dopamine head analysis misses a large portion of DANs, especially in the PAM cluster (~87 DANs

248 missed/~142 total DANs per hemisphere; Mao & Davis 2009), making it not ideal for quantifying
249 total changes in dopamine. To get around this, we recombined the *TH-GAL4* with another driver
250 that hits a large portion of the PAM cluster neurons (*GMR58E02-GAL4 (R58-GAL4)*; Jenett et al.
251 2012) generating a recombined line (labelled *TH,R58-GAL4*) that hits ~95% of DANs
252 (Supplemental Figure 4).

253 Using two different RNAi lines per gene, we microdissected adult fly brains and measured
254 dopamine for each of these 11 gene hits. Most of them did not show a consistent change in
255 dopamine levels in the brain (Figure 5E-M), but *mask* (*multiple ankyrin repeats single KH domain*)
256 and *clu* (*clueless*) knockdown showed reduction in total brain dopamine for two independent RNAi
257 lines (Figure 5N,S). While we do not have a gene trap for expression analysis for either of these
258 genes, we obtained protein trap lines (Buszczak et al. 2007; Morin et al. 2001), allowing us to
259 examine where the protein is expressed within the brain. Both Clueless and Mask are found in
260 many cells in the brain (Figure 5). When we focused on some of the DAN clusters (e.g. PPL1 and
261 PPM2), we found Clueless protein to be enriched in DANs (Figure 5P-R, P'-R'). Mask on the other
262 hand shows a broad and equal level of expression throughout most cells in the brain (Figure 5T-
263 W, U'-W').

264 In summary, our fly brain analysis revealed that while many of these genes are expressed
265 in DANs, only two of them (18%, 2/11) significantly altered dopamine in the brain, highlighting that
266 changes in head dopamine do not necessarily reflect changes in brain dopamine.

267

268 *mask* regulates Tyrosine Hydroxylase transcript and protein levels

269 First, we assessed whether reduction in dopamine caused by *clu* and *mask* knockdown
270 could be due to DAN loss. We quantified the number of DANs in major clusters (excluding the
271 PAM cluster where there is more variation in the number of DANs) based on immunostaining
272 against TH (Mao & Davis 2009). There was no difference in neuron number for any cluster
273 examined for either *clu* or *mask* knockdown (Figure 6D, Supplemental Figure 6). Next, since our

274 pigmentation gene study (Figure 1) revealed that the only enzyme in the dopamine metabolism
275 pathway that shows a significant effect on brain dopamine level upon manipulation is TH, we
276 examined if knocking down either *clu* or *mask* affects *TH* RNA or protein level. Knockdown of *clu*
277 showed an increase in TH RNA level of about 1.5-2X depending on the RNAi (Figure 6A) with no
278 effect on TH protein level (Figure 6C, Supplemental Figure 6). Interestingly, knockdown of *mask*
279 led to a significant reduction in *TH* RNA level for one RNAi (50% reduction), with the other RNAi
280 trending (20-30% reduction, Figure 6A). Upon performing immunostaining and examining TH
281 levels in different DAN clusters, two clusters showed significant reduction in TH protein level and
282 other clusters showed a trend in TH protein reduction (PAL and PPM2/3, Figure 6C, Supplemental
283 Figure 6). In conclusion, *mask* appears to reduce total dopamine levels by affecting transcription
284 of TH, while *clu* is acting through an alternative mechanism.

285 # Discussion

286 **Validation of 147 novel cuticle pigmentation genes through independent RNAi lines**

287 Our RNAi screened confirmed 153 genes that were previously implicated in *Drosophila*
288 pigmentation – 148 of these genes have not been previously associated with dopamine biology.
289 Because we observed an enrichment for genes involved in pigmentation and tyrosine metabolism
290 (Supplemental Figure 1), our method for screening and analysis effectively identified genes that
291 play critical roles in the biological process of interest.

292 While prior research has compared genes that overlap with different types of screening
293 strategies (e.g. chemical mutagenesis vs. RNAi), most RNAi phenotypes from large-scale screens
294 have not been extensively validated with alternative RNAi lines or collections. For example, in
295 Yamamoto et al, they identified 11 genes on the X chromosome with pigmentation defects from
296 an EMS (ethyl methanesulfonate) mutagenesis screen; however, of the 91 X-chromosome genes
297 identified from the RNAi screen only two of them overlapped between these screens (Yamamoto
298 et al. 2014). Both of those genes, *ATP7* and *Hr4*, were validated in our analysis. The original RNAi
299 screen used the lines available at the VDRC stock center, which includes hairpin RNAi constructs
300 (averaging ~325 base pairs) that are either random transposon mediated insertions or targeted
301 recombinase mediated insertions (Dietzl et al. 2007; Vissers et al. 2016). Alternative sources for
302 RNAi lines (i.e. TRiP and NIG) start with different backgrounds for their transgenesis, different
303 vectors for their insertion, different hairpin lengths, different insertion methods, and/or target
304 different areas of the gene (Ni et al. 2011, 2007). These differences allow researchers to
305 overcome the off-targeting seen with RNAi analysis by testing alternative lines, but to our
306 knowledge, there have been no screens or meta-analyses to systematically test consistency
307 across lines from different sources. In this analysis, we found that ~46% (153/330) of genes with
308 a pigmentation phenotype showed a phenotype in an alternative RNAi. If there were more lines
309 available for a given gene, we were more likely to see a phenotype. The genes validated had an

310 average of 2.5 additional lines available, and the genes with no pigmentation phenotype had an
311 average of 1.8 additional lines (Supplemental Figure 7). However, when we examined the number
312 of positive hits in genes with more than one RNAi line, there was very little decrease in the number
313 of positive hits (from ~77% agreement between 2 lines to ~63% agreement between 4 lines),
314 suggesting that more RNAi lines may not be necessary to identify positive phenotypes. We also
315 found 87% agreement in terms of the pigmentation color change between lines, highlighting that
316 pigmentation as a phenotype is relatively consistent (Supplemental Figure 7).

317 Interestingly, 85% of our pigmentation screen genes had at least one human homolog,
318 whereas the fly genome has ~60% conservation (1.42 fold enrichment) and genes tested in the
319 original RNAi screen list only had ~68% conservation (1.25 fold enrichment, Supplemental Figure
320 2). Similarly, there is an enrichment for disease-causing genes (51%/29%, 1.76 fold enrichment).
321 While pigmentation of the cuticle using dopamine produced through TH and Ddc is an
322 invertebrate-specific phenomenon (Yamamoto and Seto 2014), this enrichment for conserved
323 genes suggests that this phenotype is relevant for some conserved biological pathway and
324 mammalian biology. We propose that cuticle pigmentation in insects can be considered as a
325 "phenolog" (McGary et al. 2010) of certain neurological traits in mammals, a theory that requires
326 a more comprehensive investigation. Interestingly about 78% of genes with human homologs
327 from this screen are associated with a human disease with some type of neurological or
328 neurodevelopmental phenotype. This is further substantiated by the enrichment for certain GO
329 terms seen in our hits.

330

331 **Protein-protein interaction network analysis highlights unexpected gene**
332 **associations between cuticle pigmentation genes**

333 When we investigated what kind of genes were specifically found from the pigmentation
334 screen, we found some interesting trends, specifically clusters of genes that are associated with

335 ubiquitin-proteasome system (UPS), RNA processing, mitochondria, and developmental signaling
336 pathways. A number of mutations in the UPS have been linked to Parkinson's disease, but most
337 prevailing theories revolve around its effect on α-synuclein levels (Lim and Tan 2007; McKinnon
338 et al. 2020). However, there is some evidence that the UPS system regulates TH levels and
339 therefore dopamine levels in the mammalian system. For example, inhibition of the UPS system
340 has been shown to increase the TH protein levels in a PC12 rat cell line (Kawahata et al. 2015;
341 Nakashima et al. 2016). At least one TH phosphorylation site has been shown to be conserved
342 (Davis et al. 2007), and it is possible that the UPS is a conserved mechanism for regulating TH
343 levels and thus dopamine.

344 Changes in RNA processing could be indicative of changes in the dopamine synthesis
345 enzymes TH and Ddc since these enzymes undergo RNA processing to create two different
346 isoforms (Birman et al. 1994). One isoform is specific to the cuticle/epidermal and the other is
347 specific to the central nervous system. The two TH isoforms differ quite a bit in their kinetics, with
348 the epidermal isoform being generally more enzymatically active (Vié et al. 1999). In mammals,
349 post-transcriptional trafficking of TH mRNA and translational regulation has been suggested to be
350 important for its function. For example, TH mRNA gets localized to the axons for more direct
351 regulation of TH and dopamine at the axon terminal (Gervasi et al. 2016). In addition, short-term
352 stress can lead to elevated levels of TH mRNA and protein that often does not correlate with
353 transcriptional expression (Tank et al. 2008). It is also possible RNA processing factors regulate
354 dopamine levels in a non-specific manner. Global changes in RNA processing could lead to
355 cellular stress, which can significantly affect dopamine levels and dopaminergic signaling
356 (Imperato et al. 1989; Spanos et al. 2013). This may be dependent on the type of stressors since
357 while we observe a number of genes may be associated with cellular stress either directly in
358 through their molecular function from our screen (e.g. *sesB*, *Raf*, *Vps39*) (Kroemer et al. 2010;
359 Rezatabar et al. 2019; Takáts et al. 2014; Terhzaz et al. 2010; Xu et al. 2017), we did not identify
360 core components of the well-known stress pathway genes (e.g. JNK, PERK, GCN3). However, it

361 is important to note that activation of ASK1, a stress signaling integrator, is sufficient cause
362 darkening of the cuticle that is accompanied by increased expression of TH in Ddc (Sekine et al.
363 2012, 2011). Hence, our screen may not have reached saturation and there are still a number of
364 novel cuticle pigmentation genes that awaits discovery.

365 We identified 12 genes that are known to function at the mitochondria, mostly in the
366 electron transport chain (*ND-13B*, *ND-42*, *COX5A*), mitochondrial mRNA translation (*mRpL47*,
367 *mRpL48*, *CG4679*), and mitochondrial protein localization (*CG8728*, *clu*, *mask*, *Mpcp2*). It is well-
368 known that the mitochondria have a key role in dopamine metabolism in mammals since MAO
369 acts in the mitochondria to degrade dopamine. However, there is no known MOA homolog in flies,
370 and the primary mechanisms of dopamine degradation are thought to be acetylation and β-
371 alanylation that has not been linked to the mitochondria (Yamamoto and Seto 2014). Interestingly,
372 the metabolites for oxidation and methylation of dopamine (DOPAC and HVA) have been
373 observed in flies (Freeman et al. 2012; Chaudhuri et al. 2007; Wang et al. 2011; Zhang et al.
374 2005). In addition, we found mutants for enzymes that have been thought to be the primary
375 regulators of dopamine degradation (*ebony*, *tan*, and *speck*) (Wicker-Thomas and Hamann 2008;
376 Takahashi 2013) did not have any effect on dopamine in the brain (Figure 1) suggesting there is
377 either an alternative process regulating dopamine degradation in the brain. Researchers have
378 shown that pathogenic variants in *PINK1* and *PRKN* (genes that regulate mitochondrial
379 maintenance) can cause hereditary forms of Parkinson's Disease, and the drug MPTP (1-methyl-
380 4-phenyl-1,2,3,6-tetrahydropyridine) can lead to environmentally induced Parkinson's Disease,
381 by inhibiting Complex I activity and killing DANs (William Langston et al. 1983; Kitada et al. 1998;
382 Valente et al. 2004; Nicklas et al. 1985). It has been theorized that DANs are vulnerable because
383 of their structure or the potential of dopamine oxidizing within the cell (Burbulla et al. 2017), but
384 there is also some evidence that dopamine synthesis may be occurring at the mitochondria (Wang
385 et al. 2009). Our results show pigmentation can be affected by mitochondrial changes in the fruit

386 fly, and provides a molecular handle to study an unexplored novel degradation or synthesis
387 mechanism for dopamine at the mitochondria which may have relevance to human health.
388 The last major group of genes identified from our screen as a regulator of cuticle
389 pigmentation was developmental signaling, specifically EGF signaling and Hippo signaling. These
390 clusters of genes were not only clear from our network analysis, but were also identified based
391 on GO terms enrichment analysis (Supplementary Figure 1). To date, neither EGF nor Hippo
392 signaling have an established connection with dopamine biology in *Drosophila*. One reason we
393 may have pulled these genes out is because the process of forming the dorso-central thorax is
394 developmentally regulated. The thorax requires extensive remodeling from the wing imaginal disc
395 for formation, which utilizes many different key developmental signaling pathways (Letizia et al.
396 2007; Lu et al. 2022; Zeitlinger and Bohmann 1999). However, we did not identify core
397 components of the other key pathways, such as Notch or Hedgehog, suggesting that EGF and
398 Hippo are more specifically involved in this pigmentation process. We know that both EGF and
399 Hippo signaling are important to the development of the nervous system, and in mice they have
400 shown that both pathways can specifically affect the development of the dopaminergic system
401 (Yoon and Baik 2013). Since the development of most neural circuit-systems requires reiteration
402 for proper development (Pan and Monje 2020), it is plausible that EGF or Hippo signaling could
403 directly or indirectly regulate dopamine levels. Since we did not see an effect on dopamine in the
404 adult heads, this suggests that this may be developmentally specific. Overall, our pigmentation
405 screen identified unexpected pathways that could each be a potential area of pursuit in dopamine
406 metabolism since none have been explored in this context.
407

408 **Cuticle pigmentation phenotypes do not necessarily reflect changes in dopamine**

409 Biochemical analysis and pigmentation studies have established the enzymes involved in
410 dopamine metabolism in the fruit fly, but we are not aware of a research study that systematically
411 analyzed dopamine levels of classical pigmentation genes. The field has generally assumed that

412 a darker cuticle reflects an elevated level of dopamine (Massey et al. 2019; Spana et al. 2020).
413 However, when we measured dopamine from degradation enzyme mutants using the state-of-
414 the-art HPLC system, we saw either no effect on dopamine level or reduced level of dopamine in
415 the head. In addition, when we measured dopamine from the pigmentation genes from the screen,
416 a darker cuticle did not reflect elevated levels of dopamine in the head. While we were able to
417 increase dopamine by 3-5 fold upon TH cDNA overexpression in the head (Figure 4C), this
418 phenomenon was not observable in the brain. This result is a bit puzzling, considering that the
419 GAL4/UAS overexpression system typically allows one to overexpress a gene of interest well
420 outside normal conditions (often 20-30 fold mRNA expression, Goentoro et al. 2006). One reason
421 could be that there is a selective pressure or a strong feedback mechanism that prevents elevated
422 levels of dopamine in the nervous system. Since oxidized dopamine could be toxic (Zhang et al.
423 2019), this could be a mechanism to prevent cell toxicity. Another possibility is that disrupting
424 dopamine levels leads to structural changes that in turn lead to unstable dopamine. In the cuticle
425 melanin is not the only final product of dopamine; it is also used to make different types of
426 sclerotins (Sugumaran and Barek 2016). These sclerotins provide additional structural integrity to
427 the cuticle, so in theory disrupting this structural integrity could perhaps lead to increased
428 dopamine degradation, though we do not have evidence for this. Regardless, changes in cuticle
429 pigmentation do not necessarily reflect changes in dopamine level, so assumptions should not be
430 made that increase in melanin levels in the fly corresponds to increased level of dopamine. Also,
431 we found that it is generally more common to see a reduction in dopamine than an increase in
432 both the head and the brain of the fly, indicating there may be a regulatory mechanism to prevent
433 the increase of dopamine *in vivo*, which warrants further investigation.

434 Upon seeing alterations of dopamine in the head for some of the classic pigmentation
435 genes, we next wanted to test if this corresponded to changes in the brain. In the case of
436 established dopamine metabolism genes, we only saw a change in dopamine levels upon
437 reduction of TH. None of the enzymes suspected to be involved in dopamine degradation caused

438 a change in dopamine in the brain as whole-body null or strong loss-of-function mutants. When
439 we looked at expression for some of these genes, we saw that all the genes we were able to
440 assess (*black*, *speck*, *tan*) were expressed in the brain, but their expression was limited and did
441 not seem to overlap with many DANs. It may be that dopamine degradation does not happen in
442 the neurons since it was hypothesized to occur in the glia (Richardt et al. 2002; Davla et al. 2020).
443 However, the expression does not seem to show a broad glial expression using the reagents we
444 had access to. Taken together, this suggests that there is some unknown mechanism for
445 dopamine degradation in the fly brain. For the 11 genes from the pigmentation RNAi screen that
446 showed altered levels of dopamine, we assessed dopamine levels in the brain. Only 2 (18%) of
447 them showed an effect on dopamine in the brain even though several other genes are expressed
448 in DANs (ranging between 25-100% of DANs examined). This emphasizes what we found when
449 we observed in the pigmentation mutants that dopamine in the head does not necessarily reflect
450 a change in the brain. Hence, head dopamine levels should not be used as a proxy for brain
451 dopamine levels, which is sometimes used in the literature to study Parkinson disease and other
452 dopamine related disorders using *Drosophila* (Islam et al. 2012; Shimizu et al. 2020; Knight et al.
453 2014).
454

455 **_clu_ and _mask_ reduce brain dopamine levels through different mechanisms**

456 Once we identified that knockdown of *clu* and *mask* both reduced dopamine in the brain
457 without affecting the number of DANs, we hypothesized that they may be acting through TH since
458 our initial dopamine metabolism studies showed that only changes in TH significantly affected
459 dopamine levels in the brain. While these genes could also act on Ddc or other aspect of
460 dopamine homeostasis, we decided to focus on TH since this is the rate-limiting enzyme for
461 dopamine (Levitt et al. 1965) and due to reagent availability.

462 *clu* encodes a ribonucleoprotein that is thought to act at the outer mitochondrial membrane
463 to promote proper formation of different complexes that are crucial to mitochondrial function,

464 including mitophagy proteins likePink1 and Parkin (Sen et al. 2015; Wang et al. 2016). It also
465 interacts with the ribosome and translocase complex at the mitochondrial membrane (Sen et al.
466 2015; Sen and Cox 2016) suggesting it may act as a general regulator for mitochondrial protein
467 translation and import. In fact, *clu* alleles have been show to exhibit reduced ATP levels, reduced
468 mitochondrial membrane potential and elevated levels of reactive oxygen species (Sen et al.
469 2013; Yang et al. 2022). Knockdown of *clu* showed no effect on TH protein level, but since this is
470 a mitochondrial protein, it may be more likely that the effect on dopamine is through the previously
471 proposed mechanisms related to unknown roles of mitochondria to regulate dopamine levels. One
472 study proposed that dopamine synthesis can take place at the mitochondria and was regulated
473 through phosphorylation of TH (Wang et al. 2009). Hence, it is possible that while total TH protein
474 level is unaffected, post-translational status or activity of TH may be affected upon *clu* knockdown.
475 Unfortunately, we were unable to obtain an antibody that recognized phosphorylated *Drosophila*
476 TH from fly heads to test this hypothesis. Though others have been able to stain for
477 phosphorylated TH when its activity is at its peak, so it may be feasible to try additional antibodies
478 using alternative conditions (Davis et al. 2007). Considering that we observed elevated levels of
479 TH mRNA upon *clu* knockdown, some feedback mechanism may be trying to compensate for
480 reduced levels of dopamine and potentially TH activity, providing us an entry point to study such
481 feedback loop which may also involve TH phosphorylation and other signaling mechanisms
482 (Dunkley et al. 2004; Tekin et al. 2014).

483 *mask* encodes a scaffolding molecule that has been studied in a number of different
484 biological contexts (DeAngelis et al. 2020; Zhu et al. 2017; Martinez et al. 2021; Fisher et al.
485 2018). In this study, *mask* knockdown showed reduction in both *TH* mRNA and protein levels,
486 suggesting that it may reduce dopamine by reducing TH transcriptionally. Interestingly, *mask* has
487 been implicated in multiple biological pathways that were highlighted from our screen, including
488 EGF signaling (e.g. *Egfr*, *Sev*, Raf), Hippo signaling (e.g. *hpo*, *wts*, *mats*), and mitochondrial
489 biology (Sidor et al. 2013, 2019; Sansores-Garcia et al. 2013; Smith et al. 2002; Zhu et al. 2015).

490 While Egf and Hippo signaling have well-known transcriptional effects (Lusk et al. 2017; Oh and
491 Irvine 2010), whether it may regulate TH transcription directly or indirectly in this context need
492 further investigations. It is also possible that because *mask* acts in multiple of these pathways,
493 which causes it to have a strong enough effect to show a significant change in dopamine in the
494 whole brain analysis while knockdown of individual pathway genes may have a more restricted
495 role (e.g. *Egfr*, *Sos*, *hpo*). Importantly, while reduction in TH mRNA could be the primary cause of
496 decreased TH protein levels upon *mask* knockdown, additional translational or post-translational
497 mechanisms may be involved considering the pleiotropic role of Mask. Interestingly,
498 haploinsufficiency of the human ortholog of *mask* (*ANKRD17)* was recently identified as the cause
499 of a complex neurodevelopmental disorder (Chopra et al. 2021). Further investigation of whether
500 *ANKRD17* regulates dopamine levels in the mammalian brain and its mechanistic investigation
501 will likely provide a novel angle to study this understudied rare disease and related conditions.
502 In conclusion, while both of these genes caused a reduction in dopamine, they appear to
503 be acting through different mechanisms. Additional analysis on changes in enzymatic activity as
504 well as potential downstream targets would help identify exactly how these genes are acting.
505

506 **Some regulators of dopamine levels may act locally**

507 While we were able to identify two genes that significantly affect dopamine levels in the
508 brain, there were many genes that did not show a global change in the brain dopamine levels in
509 the head or brain. Also, due to the limitation in resources, we only measured dopamine in the
510 head of 35 prioritized candidates. There are still 97 conserved pigmentation genes that may affect
511 dopamine levels, some of which may function in the brain. Considering changes in head levels of
512 dopamine were not indicative of changes in brain dopamine, future experiments should be
513 prioritized based on the candidates' expression in DANs to increase the yield for novel dopamine
514 regulators.

515 In addition, when we examined the expression of some of our genes which we measured
516 dopamine levels from the head or brain (Supplemental Figure 5), we found that many of them do
517 not overlap with all DANs. Therefore, measuring global changes in dopamine may not be best for
518 determining effects on DA for many of these genes. They may require targeted dopamine
519 measurement, perhaps through a fixed or live reporter (Inagaki et al. 2012; Sun et al. 2020). It is
520 also possible to assess changes in dopamine using behavior, but this would require detailed
521 assessment for each gene since behaviors are often cluster specific (Kasture et al. 2018). For
522 example, the gene *rickets* (*rk*) is known to regulate TH activity in the cuticle, but there is no known
523 role for *rk* in adulthood. However, we found that *rk* was expressed in about ~33% of DANs in the
524 adult brain. Therefore, it may be difficult to see global changes in dopamine upon *rk* knockdown
525 considering the effect size and the degree of variability we observe in our biochemical assay, but
526 since its expression overlaps with all of the DANs in the PPL2ab cluster, we can potentially
527 measure alterations in behavior that this cluster is known to regulate, such as changes in food
528 preference (Liu et al. 2017). In conclusion, our screen of identified novel pigmentation genes, a
529 subset of which were identified as novel regulators of dopamine *in vivo*. Unbiased forward genetic
530 screens in model organisms are powerful ways to identify unanticipated links between distinct
531 biological pathways and provide new molecular handles to study the functional connections
532 between them. Application of such strategies to regulation of dopamine levels will likely continue
533 to identify novel factors, some of which will have impact on understanding the mechanism of
534 human neurological and neurodevelopmental diseases.

535 # Materials and Methods

536 **Fly Maintenance**

537 Flies (*Drosophila melanogaster*) strains and crosses were reared at 25°C on a 12:12 Light/Dark
538 (LD) program unless stated otherwise. Flies were fed a molasses-based food source. Crosses
539 were set with 3-5 males and 3-5 virgin females and transferred every two days to increase the
540 number of progenies. Different temperatures were used to achieve different levels of gene
541 knockdown or overexpression since GAL4/UAS system is temperature sensitive. The flies were
542 transferred 0-2 days post-eclosion (dpe) to separate them for age-appropriate analysis. The
543 experiments were generally run on 3-7 dpe flies unless otherwise stated.

544

545 **Fly Stocks and Crosses**

546 Mutant and transgenic trains were obtained from Bloomington *Drosophila* Stock Center (BDSC,
547 https://bdsc.indiana.edu/), Vienna Drosophila Research Center (VDRC,
548 https://www.viennabiocenter.org/vbcf/vienna-drosophila-resource-center/), the Japanese
549 National Institute of Genetics (https://shigen.nig.ac.jp/fly/nigfly/), or were gifts from scientists in
550 the field or generated in house (Supplemental Table 1-5).

551

552 For the cuticle screen *pnr-GAL4* (Calleja et al. 2000) was crossed to the specified UAS-RNAi line
553 (see Supplemental Table 1) at 29°C, 25°C, and/or 18°C and examined after pigmentation is
554 completed (>1 dpe). For the behavior and HPLC analysis *TH-GAL4* females (also called *ple-*
555 *GAL4*, BDSC stock #8848) were crossed to the specified RNAi line (see Supplemental Table).
556 For all HPLC analysis, the controls were specific to the tested UAS-RNAi line. Thus, the TRiP
557 collection of RNAi lines are compared to the *UAS-mCherry(mCh) RNAi* line (BDSC #35785) and
558 the NIG collection of RNAi lines as well as the VDRC RNAi lines are compared to the *UAS-lacZ*
559 *RNAi* line (Kennerdell and Carthew 2000). For the HPLC analysis performed on brains, we

560 recombined the *TH-GAL4* with another DAN driver *GMR58E02-GAL4* (BDSC #41347), which
561 expresses in a large group DANs in the PAM cluster (Riemensperger et al. 2013). The PAM
562 cluster of neurons are largely missed in the *TH-GAL4*, but the recombined stock captures the
563 majority of DANs (see Supplemental Figure 4). These flies are referred to as *TH,R58-GAL4*
564 throughout the article. The *TH,R58-GAL4* line was also used for qPCR and TH protein analysis
565 via immunohistochemistry.
566 For gene expression analysis *UAS-mCh::nls* (BDSC #38424) females were collected and crossed
567 with respective T2A-GAL4 lines (see Supplemental Table 5). Female and males were both
568 imaged at ~5-7dpe.
569
570 **Notum Dissection and Imaging**
571 For thorax analysis and dissection, males and females were both selected, though differences
572 were not generally observed, and females are shown here. Flies that were 3-5 dpe were collected
573 and placed in 70% EtOH. Notum dissection and imaging was performed as in (Yamamoto et al.,
574 2012). In summary, the thorax was dissected by removing the legs, abdomen, and head. Then
575 the thorax was cut such that a hole was on the ventral side to allow solution to pass into the
576 thorax. These dissected thoraces were placed in 10% KOH for 10 minutes at 90°C on a heat
577 block. Then, the KOH was removed and replaced with 70% EtOH solution. The thorax was
578 trimmed to only contain the notum (dorsal thorax), and any remaining tissue was removed. They
579 were mounted on a slide prepared with tape on two sides (to prevent the coverslip from crushing
580 the thorax) in mounting media (50% glycerol, 50% EtOH). The thoraces were imaged on a stereo
581 microscope (Leica MZ16) using OPTRONICS® MicroFIRE camera. The images are z-stack
582 brightfield images taken and collapsed using extended depth of field in Image-Pro Plus 7.0 and
583 In-Focus (Version 1.6).
584
585 **Brain Expression Analysis**

586 Brain dissections and imaging were performed as reported in (Marcogliese et al. 2022). In
587 summary, the brains were dissected at 3-7 dpe in ice cold PBS and then fixed in 4% PFA in 0.5%
588 PBST for 20 minutes. Then, they were washed with a quick wash in 0.5% PBST followed by three
589 10-20 minute washes in 0.5% PBST while on a rotator. The samples were placed in primary
590 antibody solution [anti-Tyrosine Hydroxylase 1:500, PelFreez Biologicals, rabbit, P40101 ; anti-
591 elav 1:100, Developmental Studies Hybridoma Bank, rat, 7E8A10 in solution (5% Normal Donkey
592 Serum, 0.1% NaN_3 in 0.5% PBST)] at 4°C for 3 days. Then, the samples were washed with a
593 quick wash in 0.5% PBST followed by three 10-20 minute washes in 0.5% PBST while on a
594 rotator. After the last wash, the samples were placed in a secondary antibody solution [anti-Rabbit
595 1:200 (Thermo Fisher Sci., Alexa-647, A-21208); anti-rat 1:200 (Thermo Fisher Sci., Alexa-488,
596 A-27040) in solution (5% Normal Donkey Serum, 0.1% NaN_3 in 0.5% PBST)] for two hours at
597 room temperature. The samples were washed again with one quick wash followed by three 10-
598 20 minutes washes in 0.5% PBST on a rotator. Then, the brains were mounted in Vectashield
599 mounting media and imaged on a confocal microscope (Zeiss LSM 710 or Zeiss LSM 880). All
600 images shown in this manuscript are Z-projection images that were generated using the ZEN
601 software (Zeiss).
602
603 **RNAi-based Pigmentation Screen**
604 We identified potential regulators of cuticle color from a primary screen performed in Jurgen
605 Knoblich's lab using the Vienna Drosophila Resource Center collection of RNAi lines by accessing
606 their public RNAi screening database (https://bristlescreen.imba.oeaw.ac.at/start.php). The
607 original screen was performed on 20,262 RNAi lines, encompassing 11,619 genes (~82% of
608 protein-coding genes) (Mummery-Widmer et al. 2009). We selected genes that showed a cuticle
609 pigmentation score for any RNAi line tested (selected gene scores ranged from two to ten). To
610 validate pigmentation defects, we selected genes that had RNAi lines within the Fly National
611 Institute of Genetics (NIG, 220 genes, 426 RNAi lines) or the Harvard Transgenic RNAi Project

612 (TRiP, 221 genes, 292 RNAi lines) collections. These RNAi lines were tested for a cuticle color
613 defects. Each RNAi line was tested at 29°C and 25°C. If there was no phenotype no further testing
614 was performed. If it was lethal, we tested it at 18°C.
615
616 **Classification of Cuticle Phenotypes**
617 Phenotypes were scored based on images taken for each genotype. The phenotype was scored
618 using a qualitative scoring system. This system used *UAS-TH RNAi* and *UAS-ebony RNAi*, some
619 of the strongest regulators of cuticle color, as a baseline for the "strong". Then, the other lines
620 were placed along the spectrum as mild, moderate, or strong. Phenotypes were scored by two
621 independent observers and differences were settled by a third independent observer. If there
622 was variability with one line or if there was variability amongst lines, this might appear as mild-
623 moderate, moderate-strong, or mild-strong. In these cases, the strongest phenotype observed
624 was documented as the recorded phenotype for a given gene.
625
626 **Protein-protein interaction network and gene ontology analysis**
627 The protein-protein interaction network was generated using STRING (search tool for recurring
628 instances of neighboring genes; https://string-db.org/). All of the 153 pigmentation gene hits were
629 input into multiple protein analysis for the species *Drosophila melanogaster*, and genes were
630 verified for the appropriate gene name. This database includes protein-protein interactions that
631 are physical interactions and functionally associations. For our data set we included these sources
632 of interactions: gene neighborhoods (genes that are found close together across species; (Snel
633 et al. 2000), curated databases (publicly available databases of protein interactions), and
634 experimental evidence (known complexes and pathways from curated sources) (Szklarczyk et al.
635 2021, 2023). Any genes that did not interact with other genes from our screen were not included
636 in the interaction network. This database was last accessed on 05/05/2023. The lines between
637 genes represents the confidence in the interactions. This is defined based on the strength of data

638 sources for the given interaction, which is based on complex algorithms that are dependent on
639 the source.
640 The gene ontology analysis was generated using GOrilla (Gene Ontology enRIchment anaLysis
641 and visuaLizAtion tool, https://cbl-gorilla.cs.technion.ac.il/). All of the 153 pigmentation genes hits
642 were included as target genes, and the background genes were the entire VDRC RNAi collection
643 included in the Mummery-Widmer et al. 2009 screen. Only the GO terms with a p-value greater
644 than 0.001 and a fold enrichment of greater than three were included in the analysis. Redundant
645 terms were removed using Revigo (http://revigo.irb.hr/) with a stringency of 0.7. Those that have
646 a fold enrichment greater than five were included in Supplementary Figure 1.
647
648 **Human Neurological Disease Gene Classification**
649 Homologs for each fly gene were identified using DIOPT (DRSC Integrative Ortholog Prediction
650 Tool, v8.0, https://www.flyrnai.org/diopt) (Hu et al. 2011). Genes were classified as orthologs if
651 they had a DIOPT score≥3. The human genes were scored as neurological disease-causing
652 genes if they had an OMIM (Online Mendelian Inheritance of Man, last accessed 01/01/2023,
653 https://www.omim.org/) disease association with any documented neurological phenotype
654 (Hamosh et al. 2021). Genes were also classified as human neurological disease genes if they
655 were included in the Simons Simplex Collection of Autism Spectrum Disorder gene list (last
656 accessed 06/01/2022, https://gene.sfari.org/) and had a score equal to or less than 3 (1, 2, or 3)
657 and/or syndromic (S) (Abrahams et al. 2013).
658
659 **Behavior Analysis using the *Drosophila* Activity Monitor**
660 For the behavior screen, the crosses were set in a 12:12 LD chamber at 25°C and transferred
661 every 2-3 days to increase the number of progenies. Upon eclosion, flies were transferred to 29°C
662 and kept for 2-3 more days before testing. Individual tubes (PPT5x65 Polycarbonate, Trikinetics
663 Inc, USA) appropriate for use with the *Drosophila* Activity Monitor (DAM, Model DAM2 for 5mm

664 tubes, TriKinetics Inc, USA) were loaded with approximately ½" worth of molasses-based food.
665 The end of the tube with food was sealed by placing the vial into Paraplast® (Sigma-Aldrich) wax
666 three times and allowing it to dry. Once they were dry, individual male flies were placed into each
667 vial, the vial was placed into the DAM recording chamber, and it was sealed using a 5mm tube
668 cap (CAP5, TriKinetics Inc, USA) with a hole stuffed with cotton. For each genotype, 16 individual
669 males were run, except in a few cases where we were unable to get that many flies. In which
670 case, as many living males as possible were run. The flies were loaded into a 12:12 LD chamber
671 at 29°C and monitored for 3 days. Then, the flies were removed and dead flies were eliminated
672 from analysis.
673 Locomotion and sleep analysis was run on a 24-hour period, which started at the first onset of
674 light after the flies were placed in the chamber (i.e. 18-24 hours after being placed in the chamber).
675 Locomotion was calculated based on the number of beam crossings over the full 24 hours, the
676 12 hours of light, and the 12 hours of dark. Sleep was classified as 5 minutes without any beam
677 crossings. Total Sleep was quantified as total time spent sleeping over the 12 hours of light and
678 the 12 hours of dark. Sleep latency was quantified as the amount of time after light onset or dark
679 onset before a 5 minute period of sleep. Sleep Bout Length was quantified as the average length
680 of sleep bouts (>5 minute period of sleep) during the 12 hours of light and 12 hours of dark.
681 "Outliers" were classified as lines that were more than two standard deviations from the mean of
682 all lines for any of the phenotypes scored (24 hour locomotion, 12 hour light locomotion, 12 hour
683 dark locomotion, 12 hour light total sleep, 12 hour dark total sleep, 12 hour light sleep bout length,
684 12 hour dark sleep bout length, sleep latency during the light, or sleep latency during the dark).
685 The total list of genes from all outliers was 50, which was on par with the other classifications. In
686 addition, there was not a great amount of overlap between the phenotypes scored (Figure 3) and
687 dopamine could cause an effect in potentially any of these phenotypes depending on what cells
688 the gene functions in. Thus, a gene was classified as a DAM "outlier" if it was an "outlier" in any

689 of the scored phenotypes. The data analysis of the DAM data was performed using Microsoft
690 Excel.
691
692 **High Performance Liquid Chromatography (HPLC) Analysis of dopamine and serotonin**
693 Sample Preparation
694 For the HPLC on fly heads and brain, we adapted and modified the protocol based on (Cichewicz
695 et al. 2017; Hardie and Hirsh 2006). Crosses were reared at 29°C and flies were transferred into
696 new tubes 0-2 days post eclosion (dpe). They remained at 29°C until they were 3-5 dpe. Female
697 heads were collected by anesthetizing flies with CO_2 and cutting their heads off with a razor blade.
698 Samples were collected between ZT04-ZT08. The heads were placed into 60 µL of 50 mM citrate
699 acetate (pH=4.5) and either used for analysis that day or frozen at -20°C. Five heads were used
700 per sample, and ~10 samples were run per genotype. The day of HPLC analysis, the samples
701 were thawed, grounded using a pestle for 30 seconds (Cordless Pestle Motor and Fisherbrand™
702 Disposable Pellet Pestle for 1.5mL tube). Then the samples were spun down at 13,000 rpm for
703 10 minutes. The supernatant was removed and placed into a new vial. 10 µL from each sample
704 was used for the Bradford Protein Analysis Assay. The rest of the sample solution (~40-50 µL)
705 was loaded into a vial (300 µL Polypropylene Sample Vials with 8mm Snap Caps) for HPLC
706 analysis.
707 For HPLC analysis on fly brains, flies were collected 3-7 dpe. Then, 10 fly brains (5 male, 5
708 female) were dissected in ice cold PBS. Right after dissection, the brains were transferred to 60uL
709 of ice cold 50mM citrate acetate (pH=4.5). Samples were frozen at -20°C and ran within 4 weeks
710 of collection. While not all brains were dissected for a given genotype on the same day, the
711 samples collected for each genotype compared was even for a given day (e.g. 1 control RNAi, 1
712 RNAi #1, 1 RNAi #2 OR 2 control RNAi, 2 RNAi #1, 2 RNAi #2). The day of HPLC analysis, the
713 samples were homogenized similarly to the fly heads, though for the Protein Assay, 20 µL of
714 sample was used. Then, the remaining solution was loaded for HPLC analysis.

715 Bradford Protein Analysis Assay

716 The Bio-Rad Bradford Assay was used for colorimetric scoring of total protein. See product details
717 for full description (Bio-Rad Protein Assay Kit I #5000001). Briefly, the dye reagent was diluted
718 1:4 in MilliQ H_2O. Then, the solution was filtered through a 0.22 µm SFCA Nalgene filter. A protein
719 standard was created (500 µg/mL, 250 µg/mL, 100 µg/mL, and 50 µg/mL) by diluting the protein
720 sample provided with the assay. 10 µL of each protein sample (standard or fly sample) was placed
721 into single wells of a 96-well plate. Then, 200 µL of diluted 1:4 dye reagent was added to each
722 well. The samples rested for 30-45 minutes and then absorbance was measured using BMG
723 Labtech FLUOstar OPTIMA microplate reader. Protein measurements for each sample were
724 calculated based on standards ran on the same plate.

725 HPLC Information

726 The HPLC used is a Antec® Scientific product with a LC110S pump, SYSTEC OEM MINI Vacuum
727 Degasser, AS110 autosampler, a SenCell flow cell with salt bridge reference electrode in the
728 Decade Lite. Data was collected and processed using DataApex Clarity™ chromatography
729 software. The column used is chosen to work well for neurotransmitters (Acquity UPLC BEH C18
730 Column, 130Å, 1.7 µm, 1 mm X 100 mm with Acquity In-Line 0.2 µm Filter). The mobile phase
731 was a 6% Acetonitrile mobile phase optimized for our samples (74.4 mg $NA_2EDTA{\cdot}2H_20$, 13.72
732 mL 85% w/v phosphoric acid, 42.04 g citric acid, 1.2 g OSA, 120 mL acetonitrile, H_20 up to 2L,
733 pH=6.0 using 50% NaOH solution). The mobile phase was degassed for 10 minutes using the
734 Bransonic® Ultrasonic Bath before being loaded into the HPLC machine.

735 The standards for HPLC were made by generating master stocks of 100 mM dopamine and 10
736 mM serotonin diluted in MilliQ H_2O, which were kept at 4°C. The day of HPLC analysis, the master
737 stocks were diluted to produce standards ranging from 5-100 nM for 5-HT and 5-1000 nM for
738 dopamine. Sample concentrations of dopamine (Sigma-Aldrich, Cat#H8502) and serotonin
739 (Sigma-Aldrich, Cat#H7752) were calculated based on standards run in the same batch.
740 Standards were compared to standards run on other days to assess for overall performance.

741 Standards were loaded into the 300 µL Polypropylene Sample Vials with 8mm Snap Caps for
742 HPLC analysis.
743
744 **RNA expression analysis**
745 Flies were raised at 29°C until 5-7 dpe, then heads were collected by cutting them off with a razor
746 blade. Twenty heads were collected per sample with a mixture of males and females and placed
747 directly on dry ice. Samples were kept on dry ice or at -80°C until RNA isolation. For RNA isolation
748 samples were homogenized in 200µL of TRIzol®. Then 800µL of TRIzol® was added and the
749 samples were mixed by pipetting. The samples incubated for 5 minutes at room temperature and
750 were then spun down at 12,000 rpm for 10 minutes at 4°C. The supernatant was removed and
751 200µL of chloroform was added. The samples were mixed by shaking and then incubated at room
752 temperature for 3 minutes. Then, they were spun at 10,000 rpm for 15 minutes at 4°C, and the
753 aqueous layer was collected and placed in a new tube. 500µL of isopropanol was added and the
754 samples were left to incubate for 10 minutes at room temperature. The samples were spun at
755 10,000 rpm for 10 minutes at 4°C and the supernatant was removed. The pellet was washed with
756 1mL of 75% EtOH and centrifuged at 5,000 rpm for 5 minutes. All EtOH was removed and the
757 pellet dried at room temperature for 10 minutes. Then, the pellet was dissolved in 100µL of H_2O.
758 RNA content and quality was measured using DeNovix DS-11 Fx spectrophotometer/fluorometer.
759 cDNA reverse transcription was performed according to the iScript™ reverse transcriptase Bio-
760 Rad kit and 2 µL of RNA sample was added in a 10 µL reaction for both the reverse and no
761 reverse transcriptase reaction. Samples were measured for content and quality and then they
762 were diluted to 100ng/µL. qPCR was performed using Bio-Rad iQ SYBR Green Supermix and
763 measured on Bio-Rad CFX96™ Real-Time System. The TH primers used Forward: 5'-
764 ATGTTCGCCATCAAGAAATCCT-3' and Reverse: 5'-GGGTCTCGAAACGGGCATC-3', and the
765 control primers were for Rpl32 were Forward: 5'-ATGCTAAGCTGTCGCACAAATG-3' and
766 Reverse: 5'-GTTCGATCCGTAACCGATGT-3'. For each sample, two technical replicates were

767 run for the reverse transcriptase reaction, and the final quantity was based on the average of the
768 two. If the no reverse transcriptase reaction produced a product that was a Cq within ten, the
769 sample was discarded.
770
771 **DAN and TH Quantification**
772 Samples were stained and imaged just like to the brain expression analysis, except the primarily
773 antibody solution included an Elav antibody [anti-Tyrosine Hydroxylase 1:500, PelFreez
774 Biologicals, rabbit, P40101; anti-Elav 1:100, Developmental Studies Hybridoma Bank, rat,
775 7E8A10 in solution (5% Normal Donkey Serum, 0.1% NaN_3 in 0.5% PBST)]. Confocal imaging
776 was performed as described above. Once the samples were imaged, anterior, posterior, and
777 whole brain projections were generated that included all fluorescent signals from the anterior (PAL
778 and PAM clusters) and posterior (PPL1, PPM2, PPM3, PPL2ab) neuron clusters of interest. The
779 number of neurons per cluster (excluding the PAM cluster) were counted for each sample. PPM2
780 and PPM3 clusters were counted together. For TH protein quantification samples were assessed
781 using ImageJ. A boundary was drawn around each individual cluster and quantified. Then, the
782 local background for that cluster was subtracted from the cluster to give the fluorescence for the
783 given sample. Each hemisphere was treated as a separate sample.
784
785 **Statistical Analysis**
786 Statistical analysis was performed using Graphpad Prism 10. Unless otherwise stated, all data
787 was subjected to an ROUT outlier test, where all outliers were removed, and then a one-way
788 ANOVA was performed. Each of the experimental samples were compared to the control for the
789 given samples. In the cases where there were only two samples (i.e. control and experimental),
790 a t-test was performed.

791 For the HPLC screen on heads, the samples were normalized to the controls run on that day. The
792 specific controls were specific to the given line such that the TRiP collection was normalized to
793 *UAS-mCh RNAi* control and the NIG collection was normalized to the *UAS-lacZ RNAi* control.
794

Figures and Figure Legends (Figures 1-6, Table 1)

Figure 1

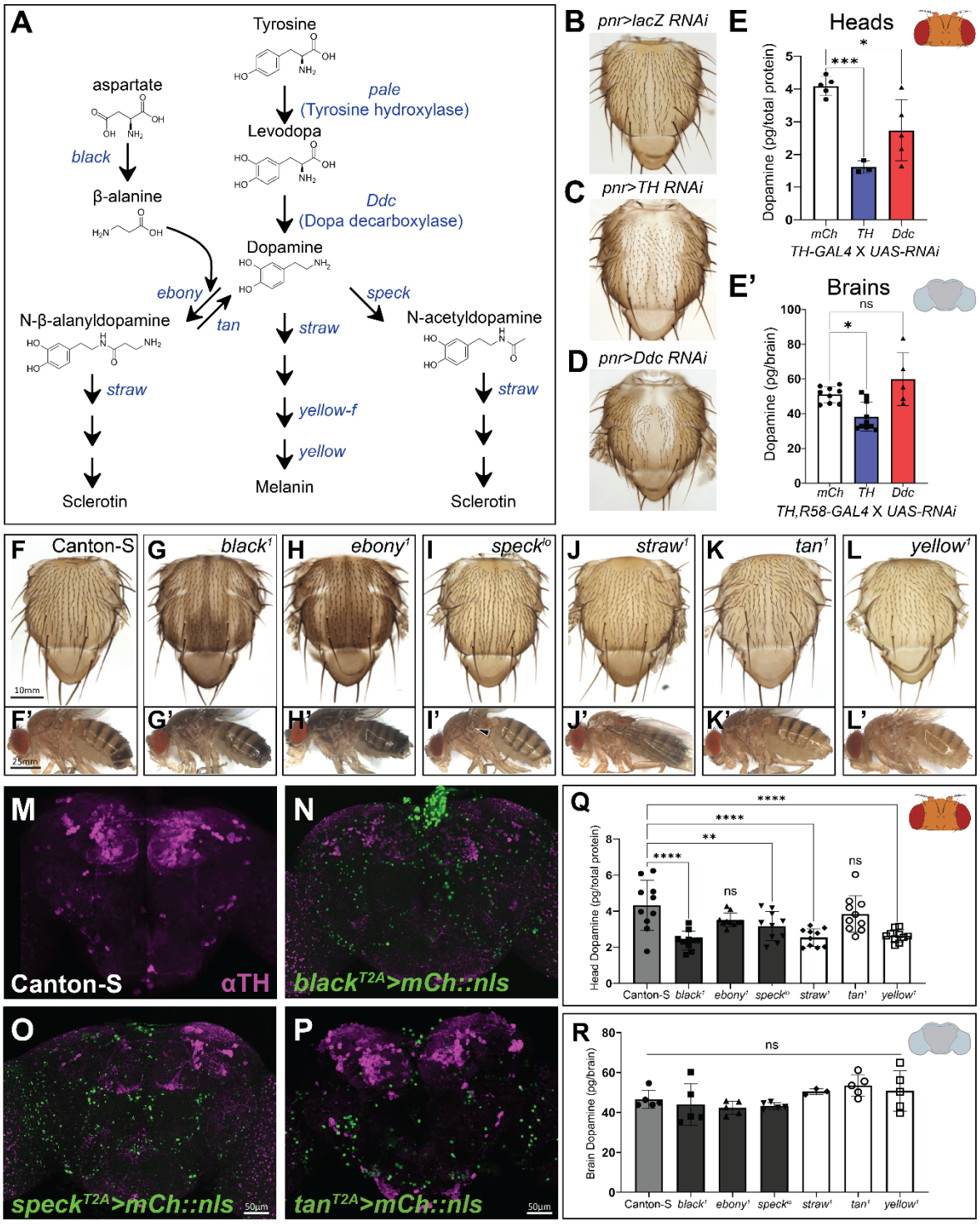

798 **Figure 1: Manipulation of most pigmentation-related enzymes do not have expected effects**
799 **on dopamine levels.** (A) Pathway for dopamine metabolism and key cuticle components. Gene
800 names encoding pigmentation-related enzymes are listed in blue font and metabolites in black
801 font, respectively. (B-D) Thorax phenotypes observed upon knockdown of synthesis enzymes
802 Tyrosine hydroxylase (TH, also known as Pale) (C), Dopa decarboxylase (Ddc) (D) compared to
803 control (B). (E-E') Dopamine levels measured from the whole head (E) and whole brain (E') upon
804 knockdown of *TH* and *Ddc*. Pigmentation phenotypes observed from cuticle pigmentation-related
805 enzymes in classical mutant alleles, as observed in the thorax (F-L) and the along the body (F'-
806 L') (Arrow in I' indicates the darker region characteristic of *speck* mutants, which is consistent with
807 previous observations). *T2A-GAL4* alleles for *black*, *speck*, and *tan* show expression in the adult
808 brain that does not have major overlap with dopaminergic neurons (DANs) (M-P). (Q) Dopamine
809 measured from the head of classical pigmentation mutants leads to reduced levels for $black^1$,
810 $ebony^1$, $straw^1$, and $yellow^1$. (R) There is no change in dopamine levels measured from dissected
811 brains of classical pigmentation mutants. Ordinary one-way ANOVA test with Dunlett multiple
812 comparisons test. *=p<0.05, **=p<0.01, ***=p<0.001, ****=p<0.0001. Error bars show standard
813 deviation (SD).

Figure 2

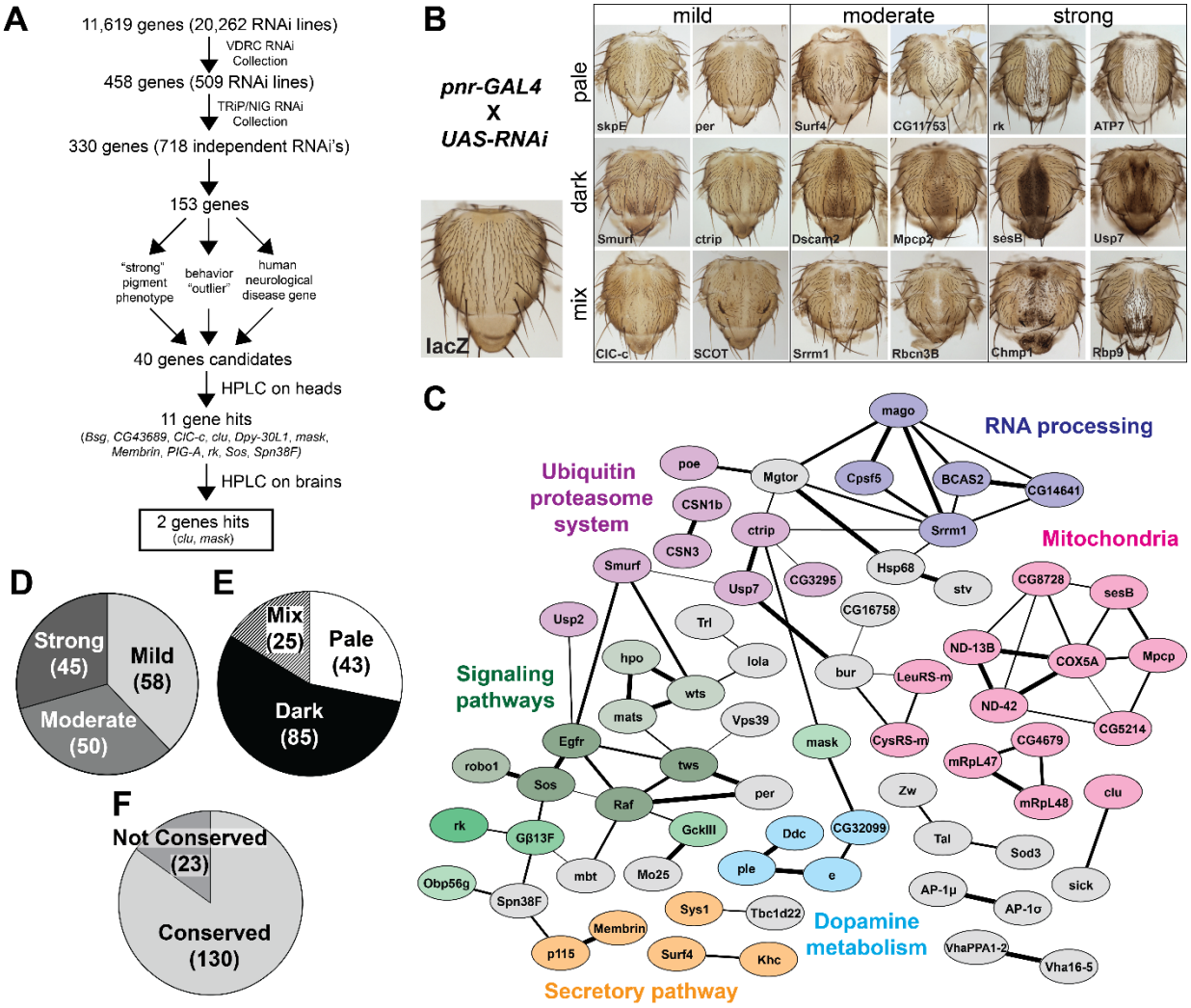
A
11,619 genes (20,262 RNAi lines)
VDRC RNAi Collection
458 genes (509 RNAi lines)
TRiP/NIG RNAi Collection
330 genes (718 independent RNAi's)
153 genes
"strong" pigment phenotype
behavior "outlier"
human neurological disease gene
40 genes candidates
HPLC on heads
11 gene hits
(Bsg, CG43689, ClC-c, clu, Dpy-30L1, mask, Membrin, PIG-A, rk, Sos, Spn38F)
HPLC on brains
2 genes hits
(clu, mask)
B
pnr-GAL4
x
UAS-RNAi
lacZ
mild
moderate
strong
pale
dark
mix
skpE
per
Surf4
CG11753
rk
ATP7
Smurf
ctrip
Dscam2
Mpcp2
sesB
Usp7
ClC-c
SCOT
Srrm1
Rbcn3B
Chmp1
Rbp9
C
RNA processing
Ubiquitin proteasome system
Mitochondria
Signaling pathways
Dopamine metabolism
Secretory pathway
mago
poe
Mgtor
Cpsf5
BCAS2
CG14641
CSN1b
ctrip
Srrm1
CSN3
Smurf
Usp7
CG3295
Hsp68
stv
CG8728
sesB
Usp2
Trl
CG16758
hpo
lola
bur
LeuRS-m
ND-13B
COX5A
Mpcp
wts
mats
Vps39
ND-42
CG5214
Egfr
mask
CysRS-m
CG4679
robo1
tws
mRpL47
Sos
per
Zw
mRpL48
clu
Raf
rk
Gβ13F
GckIII
Ddc
CG32099
Tal
Sod3
Obp56g
mbt
Mo25
ple
e
sick
Spn38F
Sys1
Tbc1d22
AP-1μ
AP-1σ
Membrin
p115
Surf4
Khc
VhaPPA1-2
Vha16-5
D
Strong (45)
Mild (58)
Moderate (50)
E
Mix (25)
Pale (43)
Dark (85)
F
Not Conserved (23)
Conserved (130)

817 **Figure 2: RNAi pigmentation screen reveals a broad spectrum of phenotypes and classes**
818 **of genes** (A) Flow chart depicting screening process for identifying novel regulators of dopamine
819 in the fly brain. (B) Examples of the breath of phenotypes observed from the RNAi-based
820 pigmentation screen for flies with 'pale', 'dark', or 'mixed' phenotypes. (C) Protein-protein
821 interaction network for 153 genes identified as high confidence pigmentation gene hits from RNAi-
822 screen using the STRING network analysis. Strength of line indicates confidence or strength of
823 data support. Interactions include gene neighborhoods, curated databases, and experimental
824 evidence as defined in the methods. Genes that do not have any known interactions with other
825 genes are not displayed. (D-F) Pie charts showing the representation for the 153 pigmentation
826 genes hits for strength of phenotype (D), phenotype color (E), and conservation (F).
827

828 **Table 1**

Fly Gene	Human Homologs with Neurological Phenotypes (DIOPT Score, Max=18)	Notable Neurological Phenotypes
AP-1sigma	AP1S2 (12), AP1S1 (11), AP2S1 (3)	seizures, ataxia, developmental delay
ATP7	ATP7A (13), ATP7B (13)	seizures, neurodegeneration, dystonia, tremor
Atu	LEO1 (10)	ASD
byn	TBXT (11), TBX19 (10)	neural tube defects, seizures
CG16758	PNP (14)	spastic diplegia, ataxia, tremor, behavioral problems
CG4328	LMX1B (10)	spina bifida
CG43689	MYT1L (7)	DD, ID
CG4679	PTCD3 (14)	psychomotor delay, myoclonus, cerebral atrophy
CG5902	AMMECR1 (13)	early motor delay, early language delay
CG8728	PMPCA (15)	ataxia
ClC-c	CLCN3 (12), CLCN4 (11), CLCNKA (3)	ID, seizures, structural abnormalities, language delay
ctrip	TRIP12 (10)	psychomotor delay, ID, delayed speech
Cyp301a1	CYP24A1 (5), CYP27B1 (4), CYP27A1 (4)	motor delay, seizures, ataxia, psychiatric symptoms
CysRS-m	CARS2 (15)	psychomotor delay, epilepsy, cerebral atrophy
Ddc	DDC (14), HDC (4)	psychomotor delay, dystonia, sleep disturbance
Dgp-1	GTPBP2 (3)	psychomotor delay, ID, ataxia, dystonia, seizures
Dscam2	DSCAM (10)	ASD
Egfr	ERBB4 (10), ERBB2 (10), ERBB3 (9)	ALS, DD, axonal neuropathy, seizures
Gbeta13F	GNB1 (15), GNB4 (13), GNB2 (12), GNB5 (3)	ID, CMT, DD, language delay, ADHD
gig	TSC2 (13)	seizures, brain structural abnormalities
Hrb98DE	HNRNPA2B1 (12), HNRNPA1 (9)	dementia, motor neuropathy, ALS
Itpr	ITPR1 (14), ITPR3 (11)	motor delay, ataxia, cerebellar atrophy
Khc	KIF5C (12), KIF5A (12)	psychomotor delay, seizures, spastic paraplegia, ALS
Larp7	LARP7 (10)	ID, DD, unstable gait, anxiety
LeuRS-m	LARS2 (15)	cognitive impairment, DD, dystonia, tremor, seizures
mask	ANKRD17 (10)	developmental delay, ID, speech delay, motor delay
mbt	PAK1 (3), PAK3 (3), PAK2 (3)	ID, macrocephaly, seizures, speech delay
Membrin	GOSR2 (13)	DD, cerebral atrophy, seizures
Mp	COL18A1 (6)	ataxia, seizures
Mpcp2	SLC25A3 (14)	motor delay
ND-13B	NDUFA5 (13)	ASD

ND-42	NDUFA10 (14)	DD, structural abnormalities
Npc2b	NPC2 (7)	DD, dementia, dystonia, seizures, behavioral problems
per	PER3 (8), PER2 (7)	sleep abnormalities
PIG-A	PIGA (15)	seizures, structural abnormalities
ple	TH (15)	ataxia, dystonia, Parkinsonism, motor and speech delay
Prosap	SHANK2 (10), SHANK3 (8)	ASD, schizophrenia, DD, seizures
Raf	BRAF (14), RAF1 (11)	DD, seizures
Rbp9	ELAVL2 (12), ELAVL3 (10)	ASD
rdx	SPOP (10)	ID, DD, speech delay
robo1	ROBO3 (8)	structural abnormalities
SCOT	OXCT1 (15)	coma, psychomotor delay
sesB	SLC25A4 (12)	motor delay, hyperreflexia
slp1	FOXG1 (6), FOXI1 (3), FOXJ1 (3), FOXC1 (3)	dystonia, motor delay, sleep and structural abnormalities
Smurf	ITCH (4), NEDD4L (3)	ID, psychomotor delay, seizures
Sod3	SOD1 (4)	ALS, spastic tetraplegia
Sos	SOS1 (14), SOS2 (12)	cognitive impair, learning disabilities
Spn38F	SERPINC1 (4), SERPINI1 (4)	seizures, dementia, cerebral atrophy
stv	BAG3 (9)	abnormal gait, neuropathy, behavioral problems
tws	PPP2R2A (13)	ataxia
Usp2	USP8 (4)	behavioral problems
Usp7	USP7 (13)	psychomotor delay, ID, seizures, structural abnormalities

Table 1: Fly pigmentation genes identified from this screen with neurological disease associated homologs in human. Human homologs were defined as fly genes with a Drosophila Integrative Orthology Prediction Tool (DIOPT, version 8.0) score greater than or equal to three for at least one human gene. Neurological disease associations were based on Online Mendelian Inheritance in Man (OMIM)_clincal disease phenotypes and high-confident ASD genes listed in Simons Foundation Autism Research Initiative (SFARI) gene database (class S, 1, 2 or 3). ASD=Autism Spectrum Disorder, DD=Developmental Delay, ID=Intellectual Disability, ALS=Amytrophic Lateral Sclerosis, CMT=Charcot-Marie-Tooth disease.

Figure 3

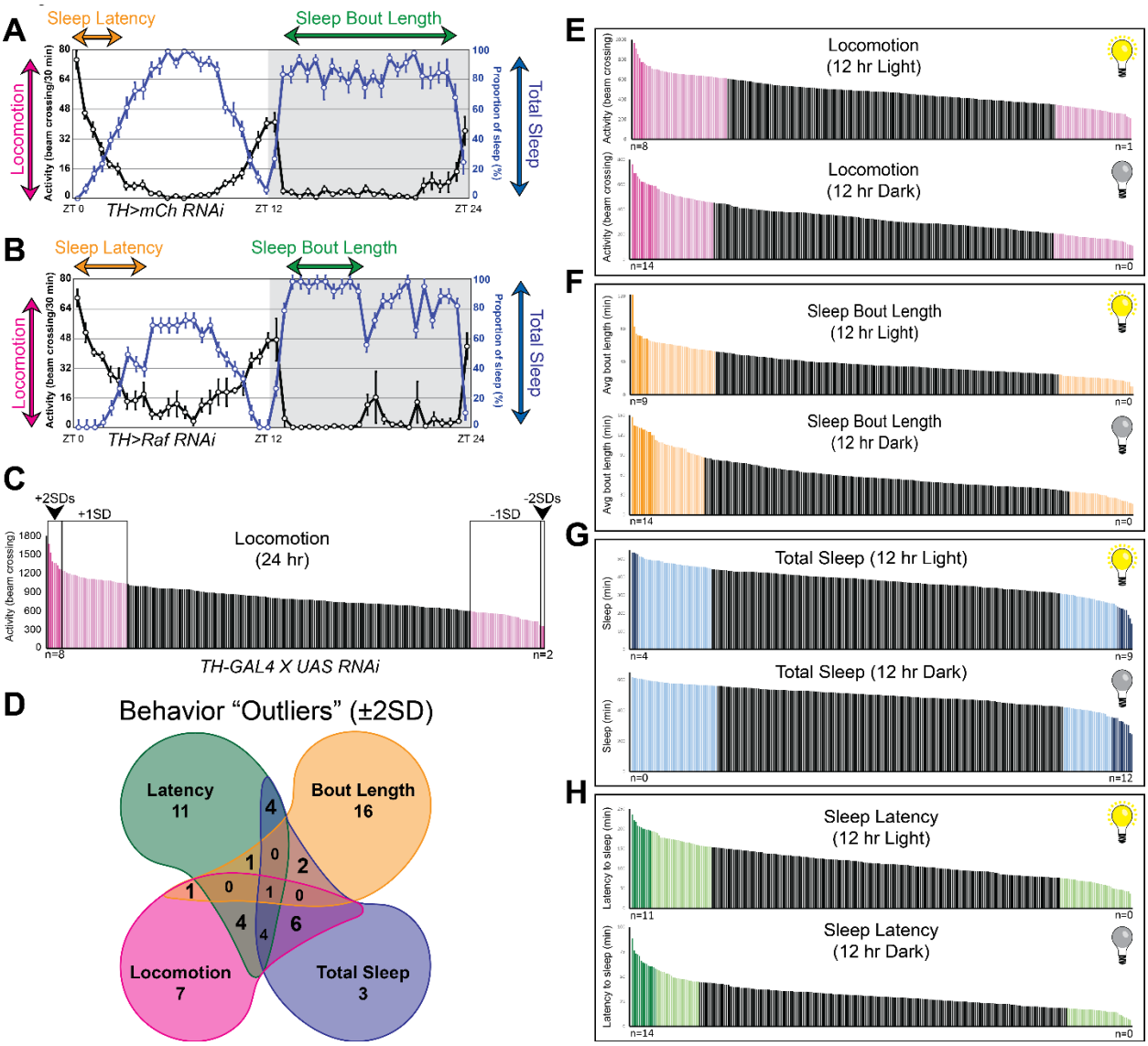
A
Sleep Latency
Sleep Bout Length
Locomotion
Total Sleep
Activity (beam crossing/30 min)
Proportion of sleep (%)
ZT 0
ZT 12
ZT 24
TH>mCh RNAi
B
Sleep Latency
Sleep Bout Length
Locomotion
Total Sleep
Activity (beam crossing/30 min)
Proportion of sleep (%)
ZT 0
ZT 12
ZT 24
TH>Raf RNAi
C
+2SDs
+1SD
-1SD
-2SDs
Locomotion
(24 hr)
Activity (beam crossing)
n=8
n=2
TH-GAL4 X UAS RNAi
D
Behavior "Outliers" (±2SD)
Latency
11
Bout Length
16
Locomotion
7
Total Sleep
3
4
0
1
2
1
0
1
0
4
4
6
E
Locomotion
(12 hr Light)
Locomotion
(12 hr Dark)
Activity (beam crossing)
n=8
n=1
n=14
n=0
F
Sleep Bout Length
(12 hr Light)
Sleep Bout Length
(12 hr Dark)
Avg bout length (min)
n=9
n=0
n=14
n=0
G
Total Sleep (12 hr Light)
Total Sleep (12 hr Dark)
Sleep (min)
n=4
n=9
n=0
n=12
H
Sleep Latency
(12 hr Light)
Sleep Latency
(12 hr Dark)
Latency to sleep (min)
n=11
n=0
n=14
n=0

842 **Figure 3: *Drosophila* Activity Monitor (DAM)-based screen identifies 60 lines**
843 **corresponding to 45 genes as behavioral "outliers".** Activity and sleep data showing
844 representative quantification for the phenotypes measured in a neutral RNAi line (*mCherry RNAi*,
845 A) and an example of a behavioral "outlier" (*Raf RNAi*, B) knocked down in many dopaminergic
846 cells (*TH-GAL4*). (C) Bar graph showing range of all RNAi lines tested for 24hr locomotion
847 phenotype, where light pink represents lines ±1SD away from the mean, and dark pink are lines
848 ±2SDs away from the mean (a.k.a. "outliers"). (D) Venn diagram for all "outliers" identified for the
849 four phenotypes examined (sleep latency, sleep bout length, locomotion, and total sleep). (E-H)
850 Bar graphs showing range of RNAi lines tested for locomotion (E), sleep bout length (F), total
851 sleep (G), and sleep latency (H).

852

853 **Figure 4**

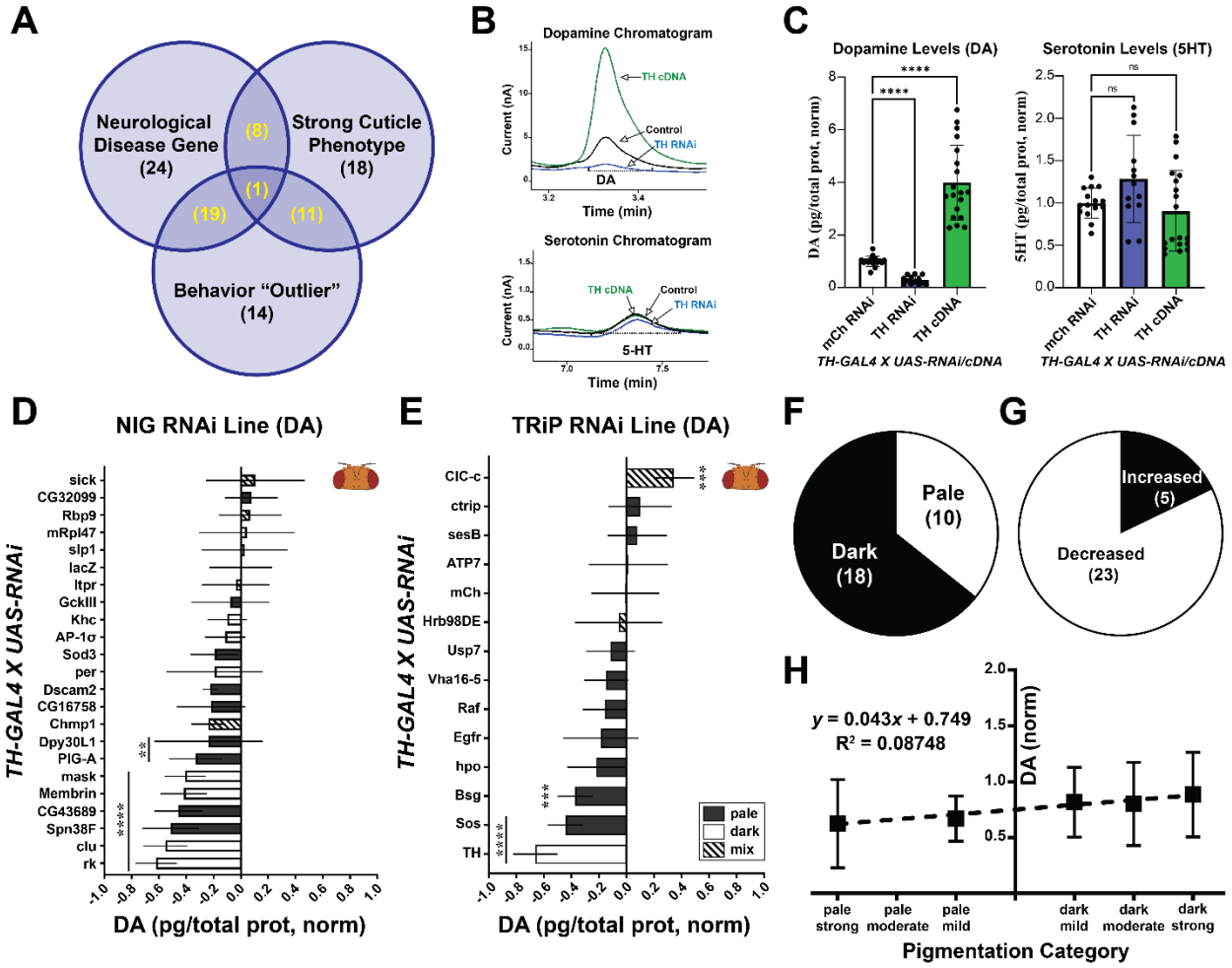

854

855

856 **Figure 4: Eleven genes with altered levels of head dopamine upon knockdown.** (A) Venn
857 diagram showing three categories that were used to prioritze 39 genes (in yellow) tested for
858 altered levels of dopamine. (B) Representative chromatograms showing peaks for dopamine and
859 serotonin for upon knockdown or overexpression of TH in many dopaminergic cells (*TH-GAL4*).
860 (C) Quantification of dopamine (DA) and serotonin (5-HT) using HPLC upon knockdown (*TH>TH*
861 *RNAi*, blue) or overexpression of (*TH>TH cDNA*, green) of TH. (D-E) HPLC analysis on prioritized
862 gene hits for lines from the NIG (D) or the TRiP (E) collection of UAS-RNAi lines. Pie charts for
863 the prioritized genes hits (39 genes) showing the representation of cuticle color (F) and the trend
864 of change in dopamine (G). (H) XY plot showing pigmentation phenotype compared to dopamine
865 levels observed. Brown-Forsythe test showed different SDs for (C), so Brown-Forsythe ANOVA
866 test performed with Dunnett's T3 multiple comparisons test. For (D) and (E) ordinary One-way
867 ANOVA test with Dunnett's multiple comparisons test. **=p<0.01, ***=p<0.001, ****=p<0.0001.
868 Error bars represent SD.

869

870 **Figure 5**

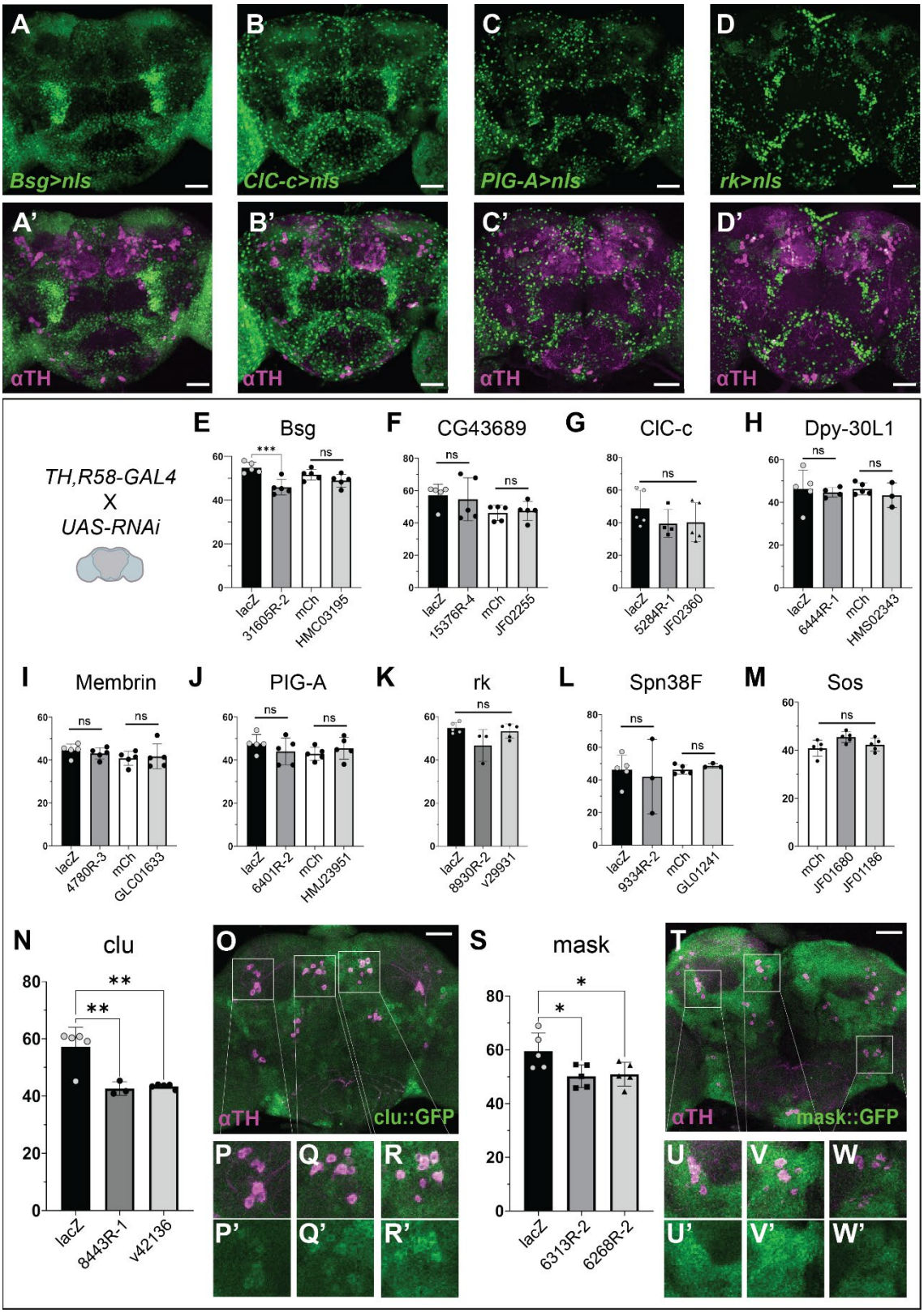

871

872 **Figure 5: Analysis of 11 genes identifies *mask* and *clu* as novel regulators of dopamine**
873 **levels in the fly brain** (A-D) *Bsg^{T2A}-GAL4*, *ClC-c^{T2A}-GAL4*, *PIG-A^{T2A}-GAL4*, and *rk^{T2A}-GAL4*
874 driving *UAS-mCh::nls* (nuclear localized mCherry) shows broad expression patterns in the brain.
875 (A'-D') These expression patterns overlaps with some to many dopaminergic neurons. Dopamine
876 measured from dissected adult brains upon knockdown of *Bsg* (E), *CG43689* (F), *ClC-c* (G), *Dpy-*
877 *30L1* (H), *Membrin* (I), *PIG-A* (J), *rk* (K), *Spn38F* (L), *Sos* (M) do not show consistent changes in
878 dopamine using a novel recombined doaminergic GAL4 driver (*TH, R58-GAL4*). (N) Knockdown
879 of *clu* shows consistent reduction in total dopamine in the adult fly brain. (O) *clu::GFP* shows
880 broad expression in the brain and may be enriched in many DANs (P-R, P-R'). (S) Knockdown of
881 *mask* shows consistent reduction in total dopamine in the adult fly brain. (T) *mask::GFP* shows
882 broad expression in the brain and overlaps with many DANs (U-W, U'-W'). For samples with one
883 control to one RNAi, t-tests were performed (E, F, H, I, J, L). For samples with two samples for
884 one control, ordinary one-way ANOVA was done with Dunnett's multiple comparisons test (G, K,
885 M, R, W). Error bars represent SD. Scale bars are 50 μm.

886

887 **Figure 6**

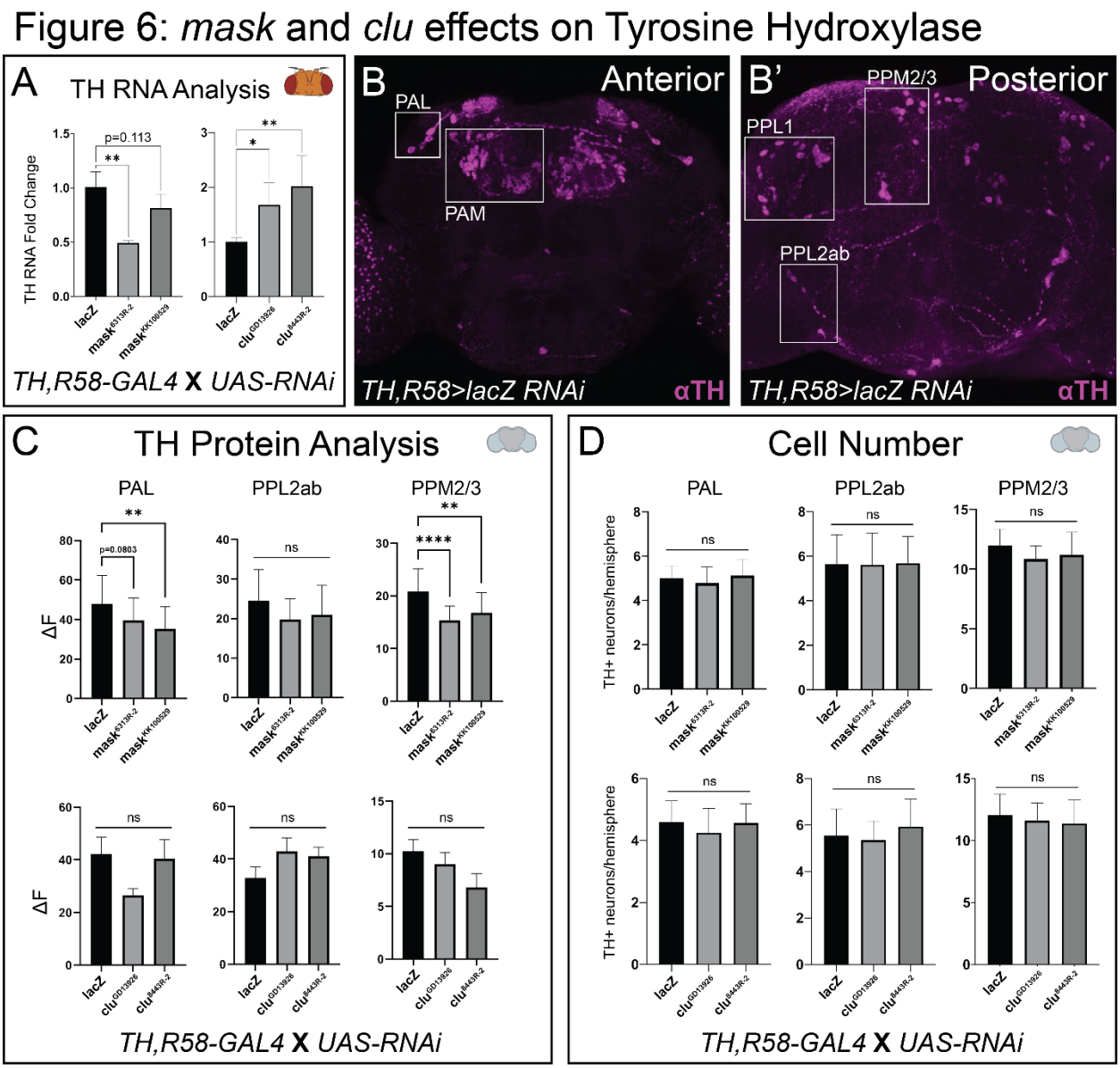

888

889

890 **Figure 6: *mask* and *clu* knockdown do not affect TH cell number and having different**
891 **affects TH levels** (A) qRT-PCR of TH upon *mask* and *clu* knockdown shows reduced TH mRNA
892 upon *mask* knockdown and increased TH mRNA upon *clu* knockdown using the recombined
893 dopaminergic (*TH, R58-GAL4*) driver. (B-B') Image showing the primary clusters of DANs in the
894 anterior (B) and posterior (B') of the adult fly brain. (C) Quantification of total TH protein level
895 through immunofluorescence signals in given clusters of DANs upon knockdown of *mask* and *clu*.
896 (D) Quantification of the number of TH positive (TH+) neurons in given clusters of DANs upon
897 knockdown of *mask* and *clu*. Ordinary one-way ANOVAs performed with Dunnett's multiple
898 comparisons for those with significant differences. *=$p<0.05$, **$p<0.01$, ****$p<0.0001$. Error bars
899 represent SD.
900

Acknowledgements

This work was supported by startup funds to SY from the Jan and Dan Duncan Neurological Research Institute at Texas Children's Hospital and the Department of Molecular and Human Genetics at Baylor College of Medicine. Confocal microscopy at BCM was supported in part by the Intellectual and Developmental Disabilities Research Center (IDDRC, grant number U54HD083092) from the Eunice Kennedy Shriver National Institute of Child Health & Human Development. We thank the Bloomington *Drosophila* Stock Center (USA), the National Institutes Genetics Fly Stock Center (Japan), *Vienna* Drosophila RNAi Center (Austria) and Dr. Hugo Bellen for providing useful fly stocks and reagents for this project. We would like to thank Drs. Jonathan Andrews, Hugo Bellen, Brigitte Dauwalder, Herman Dierick, Linsday Goodman, Oguz Kanca, Kartik Venkatachalam, Michael Wangler, Sheng Zhang and Huda Zoghbi for useful suggestions, discussions and advice on the overall project.

914 # References

915 Abrahams, B.S., Arking, D.E., Campbell, D.B., Mefford, H.C., Morrow, E.M., Weiss, L.A., et al.
916 (2013). SFARI Gene 2.0: A Community-Driven Knowledgebase for the Autism Spectrum
917 Disorders (ASDs). Mol. Autism 4 (1). doi: 10.1186/2040-2392-4-36.
918 Armstrong, M.J., and Okun, M.S. (2020). Diagnosis and Treatment of Parkinson Disease: A
919 Review. JAMA 323 (6): 548–60. doi: 10.1001/JAMA.2019.22360.
920 Bayersdorfer, F., Voigt, A., Schneuwly, S., and Botella, J.A. (2010). Dopamine-Dependent
921 Neurodegeneration in Drosophila Models of Familial and Sporadic Parkinson's Disease.
922 Neurobiol. Dis. 40 (1): 113–19. doi: 10.1016/J.NBD.2010.02.012.
923 Birman, S., Morgan, B., Anzivino, M., and Hirsh, J. (1994). A Novel and Major Isoform of
924 Tyrosine Hydroxylase in Drosophila Is Generated by Alternative RNA Processing. J. Biol.
925 Chem. 269 (42): 26559–67. doi: 10.1016/S0021-9258(18)47231-6.
926 Brand, A.H., and Perrimon, N. (1993). Targeted Gene Expression as a Means of Altering Cell
927 Fates and Generating Dominant Phenotypes. Development 118 (2): 401–15.
928 http://www.ncbi.nlm.nih.gov/pubmed/8223268.
929 Budnik, V., and White, K. (1987). Genetic Dissection of Dopamine and Serotonin Synthesis in
930 the Nervous System of Drosophila Melanogaster. J. Neurogenet. 4 (6): 309–14. doi:
931 10.3109/01677068709167191.
932 Burbulla, L.F., Song, P., Mazzulli, J.R., Zampese, E., Wong, Y.C., Jeon, S., et al. (2017).
933 Dopamine Oxidation Mediates Mitochondrial and Lysosomal Dysfunction in Parkinson's
934 Disease. Science 357 (6357): 1255–61. doi: 10.1126/SCIENCE.AAM9080.
935 Buszczak, M., Paterno, S., Lighthouse, D., Bachman, J., Planck, J., Owen, S., et al. (2007). The
936 Carnegie Protein Trap Library: A Versatile Tool for Drosophila Developmental Studies.
937 Genetics 175 (3): 1505–31. doi: 10.1534/GENETICS.106.065961.
938 Calleja, M., Herranz, H., Estella, C., Casal, J., Lawrence, P., Simpson, P., et al. (2000).

939 Generation of Medial and Lateral Dorsal Body Domains by the Pannier Gene of
940 Drosophila. Development 127 (18): 3971–80. doi: 10.1242/DEV.127.18.3971.
941 Chaudhuri, A., Bowling, K., Funderburk, C., Lawal, H., Inamdar, A., Wang, Z., et al. (2007).
942 Interaction of Genetic and Environmental Factors in a Drosophila Parkinsonism Model. J.
943 Neurosci. 27 (10): 2457. doi: 10.1523/JNEUROSCI.4239-06.2007.
944 Chiu, J.C., Low, K.H., Pike, D.H., Yildirim, E., and Edery, I. (2010). Assaying Locomotor Activity
945 to Study Circadian Rhythms and Sleep Parameters in Drosophila. J. Vis. Exp., no. 43. doi:
946 10.3791/2157.
947 Chopra, M., McEntagart, M., Clayton-Smith, J., Platzer, K., Shukla, A., Girisha, K.M., et al.
948 (2021). Heterozygous ANKRD17 Loss-of-Function Variants Cause a Syndrome with
949 Intellectual Disability, Speech Delay, and Dysmorphism. Am. J. Hum. Genet. 108 (6):
950 1138–50. doi: 10.1016/J.AJHG.2021.04.007.
951 Church, F.C. (2021). Treatment Options for Motor and Non-Motor Symptoms of Parkinson's
952 Disease. Biomolecules 11 (4). doi: 10.3390/BIOM11040612.
953 Cichewicz, K., Garren, E.J., Adiele, C., Aso, Y., Wang, Z., Wu, M., et al. (2017). A New Brain
954 Dopamine-Deficient Drosophila and Its Pharmacological and Genetic Rescue. Genes.
955 Brain. Behav. 16 (3): 394–403. doi: 10.1111/GBB.12353.
956 Clark, I.E., Dodson, M.W., Jiang, C., Cao, J.H., Huh, J.R., Seol, J.H., et al. (2006). Drosophila
957 Pink1 Is Required for Mitochondrial Function and Interacts Genetically with Parkin. Nature
958 441 (7097): 1162–66. doi: 10.1038/nature04779.
959 Davis, M.M., O'Keefe, S.L., Primrose, D.A., and Hodgetts, R.B. (2007). A Neuropeptide
960 Hormone Cascade Controls the Precise Onset of Post-Eclosion Cuticular Tanning in
961 Drosophila Melanogaster. Development 134 (24): 4395–4404. doi: 10.1242/DEV.009902.
962 Davla, S., Artiushin, G., Li, Y., Chitsaz, D., Li, S., Sehgal, A., et al. (2020). AANAT1 Functions in
963 Astrocytes to Regulate Sleep Homeostasis. Elife 9 (September): 1–48. doi:
964 10.7554/ELIFE.53994.

965 DeAngelis, M.W., McGhie, E.W., Coolon, J.D., and Johnson, R.I. (2020). Mask, a Component of
966 the Hippo Pathway, Is Required for Drosophila Eye Morphogenesis. Dev. Biol. 464 (1): 53–
967 70. doi: 10.1016/J.YDBIO.2020.05.002.
968 Diao, F., Ironfield, H., Luan, H., Diao, F., Shropshire, W.C., Ewer, J., et al. (2015). Plug-and-
969 Play Genetic Access to Drosophila Cell Types Using Exchangeable Exon Cassettes. Cell
970 Rep. 10 (8): 1410–21. doi: 10.1016/j.celrep.2015.01.059.
971 Dietzl, G., Chen, D., Schnorrer, F., Su, K.C., Barinova, Y., Fellner, M., et al. (2007). A Genome-
972 Wide Transgenic RNAi Library for Conditional Gene Inactivation in Drosophila. Nature 448
973 (7150): 151–56. doi: 10.1038/NATURE05954.
974 Dunkley, P.R., Bobrovskaya, L., Graham, M.E., Nagy-Felsobuki, E.I. Von, and Dickson, P.W.
975 (2004). Tyrosine Hydroxylase Phosphorylation: Regulation and Consequences. J.
976 Neurochem. 91 (5): 1025–43. doi: 10.1111/J.1471-4159.2004.02797.X.
977 Fisher, K.H., Fragiadaki, M., Pugazhendhi, D., Bausek, N., Arredondo, M.A., Thomas, S.J., et
978 al. (2018). A Genome-Wide RNAi Screen Identifies MASK as a Positive Regulator of
979 Cytokine Receptor Stability. J. Cell Sci. 131 (13). doi: 10.1242/JCS.209551.
980 Freeman, A., Pranski, E., Miller, R.D., Radmard, S., Bernhard, D., Jinnah, H.A., et al. (2012).
981 Sleep Fragmentation and Motor Restlessness in a Drosophila Model of Restless Legs
982 Syndrome. Curr. Biol. 22 (12): 1142. doi: 10.1016/J.CUB.2012.04.027.
983 Frighetto, G., Zordan, M.A., Castiello, U., Megighian, A., and Martin, J.R. (2022). Dopamine
984 Modulation of Drosophila Ellipsoid Body Neurons, a Nod to the Mammalian Basal Ganglia.
985 Front. Physiol. 13 (April). doi: 10.3389/FPHYS.2022.849142.
986 Gervasi, N., Tchénio, P., and Preat, T. (2010). PKA Dynamics in a Drosophila Learning Center:
987 Coincidence Detection by Rutabaga Adenylyl Cyclase and Spatial Regulation by Dunce
988 Phosphodiesterase. Neuron 65 (4): 516–29. doi: 10.1016/J.NEURON.2010.01.014.
989 Gervasi, N.M., Scott, S.S., Aschrafi, A., Gale, J., Vohra, S.N., Macgibeny, M.A., et al. (2016).
990 The Local Expression and Trafficking of Tyrosine Hydroxylase MRNA in the Axons of

991 Sympathetic Neurons. RNA 22 (6): 883–95. doi: 10.1261/RNA.053272.115.
992 Goentoro, L.A., Yakoby, N., Goodhouse, J., Schüpbach, T., and Shvartsman, S.Y. (2006).
993 Quantitative Analysis of the GAL4/UAS System in Drosophila Oogenesis. Genesis 44 (2):
994 66–74. doi: 10.1002/GENE.20184.
995 Grace, A.A. (2016). Dysregulation of the Dopamine System in the Pathophysiology of
996 Schizophrenia and Depression. Nat. Rev. Neurosci. 17 (8): 524–32. doi:
997 10.1038/NRN.2016.57.
998 Hamosh, A., Amberger, J.S., Bocchini, C., Scott, A.F., and Rasmussen, S.A. (2021). Online
999 Mendelian Inheritance in Man (OMIM®): Victor McKusick's Magnum Opus. Am. J. Med.
1000 Genet. A 185 (11): 3259–65. doi: 10.1002/AJMG.A.62407.
1001 Hardie, S.L., and Hirsh, J. (2006). An Improved Method for the Separation and Detection of
1002 Biogenic Amines in Adult Drosophila Brain Extracts by High Performance Liquid
1003 Chromatography. J. Neurosci. Methods 153 (2): 243–49. doi:
1004 10.1016/J.JNEUMETH.2005.11.001.
1005 Heisenberg, M., Borst, A., Wagner, S., and Byers, D. (1985). Drosophila Mushroom Body
1006 Mutants Are Deficient in Olfactory Learning. J. Neurogenet. 2 (1): 1–30. doi:
1007 10.3109/01677068509100140.
1008 Hovemann, B.T., Ryseck, R.P., Walldorf, U., Störtkuhl, K.F., Dietzel, I.D., and Dessen, E.
1009 (1998). The Drosophila Ebony Gene Is Closely Related to Microbial Peptide Synthetases
1010 and Shows Specific Cuticle and Nervous System Expression. Gene 221 (1): 1–9. doi:
1011 10.1016/S0378-1119(98)00440-5.
1012 Hu, Y., Flockhart, I., Vinayagam, A., Bergwitz, C., Berger, B., Perrimon, N., et al. (2011). An
1013 Integrative Approach to Ortholog Prediction for Disease-Focused and Other Functional
1014 Studies. BMC Bioinformatics 12 (August). doi: 10.1186/1471-2105-12-357.
1015 Imperato, A., Puglisi-Allegra, S., Casolini, P., Zocchi, A., and Angelucci, L. (1989). Stress-
1016 Induced Enhancement of Dopamine and Acetylcholine Release in Limbic Structures: Role

1017 of Corticosterone. Eur. J. Pharmacol. 165 (2–3): 337–38. doi: 10.1016/0014-
1018 2999(89)90735-8.
1019 Inagaki, H.K., Ben-Tabou De-Leon, S., Wong, A.M., Jagadish, S., Ishimoto, H., Barnea, G., et
1020 al. (2012). Visualizing Neuromodulation In Vivo: TANGO-Mapping of Dopamine Signaling
1021 Reveals Appeptite Control of Sugar Sensing. Cell 148 (3): 583. doi:
1022 10.1016/J.CELL.2011.12.022.
1023 Islam, R., Yang, L., Sah, M., Kannan, K., Anamani, D., Vijayan, C., et al. (2012). A
1024 Neuroprotective Role of the Human Uncoupling Protein 2 (HUCP2) in a Drosophila
1025 Parkinson's Disease Model. Neurobiol. Dis. 46 (1): 137–46. doi:
1026 10.1016/J.NBD.2011.12.055.
1027 Janssens, J., Aibar, S., Taskiran, I.I., Ismail, J.N., Gomez, A.E., Aughey, G., et al. (2022).
1028 Decoding Gene Regulation in the Fly Brain. Nature 601 (7894): 630–36. doi:
1029 10.1038/S41586-021-04262-Z.
1030 Jenett, A., Rubin, G.M., Ngo, T.T.B., Shepherd, D., Murphy, C., Dionne, H., et al. (2012). A
1031 GAL4-Driver Line Resource for Drosophila Neurobiology. Cell Rep. 2 (4): 991–1001. doi:
1032 10.1016/J.CELREP.2012.09.011.
1033 Kanca, O., Zirin, J., Garcia-Marques, J., Knight, S.M., Yang-Zhou, D., Amador, G., et al. (2019).
1034 An Efficient CRISPR-Based Strategy to Insert Small and Large Fragments of DNA Using
1035 Short Homology Arms. Elife 8 (November). doi: 10.7554/ELIFE.51539.
1036 Kasture, A.S., Hummel, T., Sucic, S., and Freissmuth, M. (2018). Big Lessons from Tiny Flies:
1037 Drosophila Melanogaster as a Model to Explore Dysfunction of Dopaminergic and
1038 Serotonergic Neurotransmitter Systems. Int. J. Mol. Sci. 19 (6). doi:
1039 10.3390/IJMS19061788.
1040 Kawahata, I., Ohtaku, S., Tomioka, Y., Ichinose, H., and Yamakuni, T. (2015). Dopamine or
1041 Biopterin Deficiency Potentiates Phosphorylation at (40)Ser and Ubiquitination of Tyrosine
1042 Hydroxylase to Be Degraded by the Ubiquitin Proteasome System. Biochem. Biophys.

1043 Res. Commun. 465 (1): 53–58. doi: 10.1016/J.BBRC.2015.07.125.
1044 Kennerdell, J.R., and Carthew, R.W. (2000). Heritable Gene Silencing in Drosophila Using
1045 Double-Stranded RNA. Nat. Biotechnol. 18 (8): 896–98. doi: 10.1038/78531.
1046 Kitada, T., Asakawa, S., Hattori, N., Matsumine, H., Yamamura, Y., Minoshima, S., et al. (1998).
1047 Mutations in the Parkin Gene Cause Autosomal Recessive Juvenile Parkinsonism. Nature
1048 392 (6676): 605–8. doi: 10.1038/33416.
1049 Knight, A.L., Yan, X., Hamamichi, S., Ajjuri, R.R., Mazzulli, J.R., Zhang, M.W., et al. (2014). The
1050 Glycolytic Enzyme, GPI, Is a Functionally Conserved Modifier of Dopaminergic
1051 Neurodegeneration in Parkinson's Models. Cell Metab. 20 (1): 145–57. doi:
1052 10.1016/J.CMET.2014.04.017.
1053 Kroemer, G., Mariño, G., and Levine, B. (2010). Autophagy and the Integrated Stress
1054 Response. Mol. Cell 40 (2): 280. doi: 10.1016/J.MOLCEL.2010.09.023.
1055 Lee, P.-T., Zirin, J., Kanca, O., Lin, W.-W., Schulze, K.L., Li-Kroeger, D., et al. (2018). A Gene-
1056 Specific T2A-GAL4 Library for Drosophila. Elife 7 (March). doi: 10.7554/eLife.35574.
1057 Letizia, A., Bario, R., and Campuzano, S. (2007). Antagonistic and Cooperative Actions of the
1058 EGFR and Dpp Pathways on the Iroquois Genes Regulate Drosophila Mesothorax
1059 Specification and Patterning. Development 134 (7): 1337–46. doi: 10.1242/DEV.02823.
1060 Levitt, M., Spector, S., Sjoerdsma, A., and Udenfriend, S. (1965). ELUCIDATION OF THE
1061 RATE-LIMITING STEP IN NOREPINEPHRINE BIOSYNTHESIS IN THE PERFUSED
1062 GUINEA-PIG HEART. J. Pharmacol. Exp. Ther. 148 (1).
1063 Li, H., Janssens, J., Waegeneer, M. de, Kolluru, S.S., Davie, K., Gardeux, V., et al. (2022). Fly
1064 Cell Atlas: A Single-Nucleus Transcriptomic Atlas of the Adult Fruit Fly. Science (80-.). 375
1065 (6584). doi:
1066 10.1126/SCIENCE.ABK2432/SUPPL_FILE/SCIENCE.ABK2432_MDAR_REPRODUCIBILI
1067 TY_CHECKLIST.PDF.
1068 Lim, K.L., and Tan, J.M.M. (2007). Role of the Ubiquitin Proteasome System in Parkinson's

1069 Disease. BMC Biochem. 8 (Suppl 1): S13. doi: 10.1186/1471-2091-8-S1-S13.
1070 Liu, Q., Tabuchi, M., Liu, S., Kodama, L., Horiuchi, W., Daniels, J., et al. (2017). Branch-Specific
1071 Plasticity of a Bifunctional Dopamine Circuit Encodes Protein. Science 356 (6337): 534.
1072 doi: 10.1126/SCIENCE.AAL3245.
1073 Livingstone, M.S., and Tempel, B.L. (1983). Genetic Dissection of Monoamine Neurotransmitter
1074 Synthesis in Drosophila. Nature 303 (5912): 67–70. doi: 10.1038/303067A0.
1075 López-Cruz, L., San Miguel, N., Carratalá-Ros, C., Monferrer, L., Salamone, J.D., and Correa,
1076 M. (2018). Dopamine Depletion Shifts Behavior from Activity Based Reinforcers to More
1077 Sedentary Ones and Adenosine Receptor Antagonism Reverses That Shift: Relation to
1078 Ventral Striatum DARPP32 Phosphorylation Patterns. Neuropharmacology 138 (August):
1079 349–59. doi: 10.1016/J.NEUROPHARM.2018.01.034.
1080 Lu, J., Wang, Y., Wang, X., Wang, D., Pflugfelder, G.O., and Shen, J. (2022). The Tbx6
1081 Transcription Factor Dorsocross Mediates Dpp Signaling to Regulate Drosophila Thorax
1082 Closure. Int. J. Mol. Sci. 23 (9). doi: 10.3390/IJMS23094543.
1083 Lusk, J.B., Lam, V.Y.M., and Tolwinski, N.S. (2017). Epidermal Growth Factor Pathway
1084 Signaling in Drosophila Embryogenesis: Tools for Understanding Cancer. Cancers (Basel).
1085 9 (2). doi: 10.3390/CANCERS9020016.
1086 Mao, Z., and Davis, R.L. (2009). Eight Different Types of Dopaminergic Neurons Innervate the
1087 Drosophila Mushroom Body Neuropil: Anatomical and Physiological Heterogeneity. Front.
1088 Neural Circuits 3 (JUL): 5. doi: 10.3389/NEURO.04.005.2009/BIBTEX.
1089 Marcogliese, P.C., Deal, S.L., Andrews, J., Harnish, J.M., Bhavana, V.H., Graves, H.K., et al.
1090 (2022). Drosophila Functional Screening of de Novo Variants in Autism Uncovers
1091 Damaging Variants and Facilitates Discovery of Rare Neurodevelopmental Diseases. Cell
1092 Rep. 38 (11). doi: 10.1016/J.CELREP.2022.110517.
1093 Martinez, D., Zhu, M., Guidry, J.J., Majeste, N., Mao, H., Yanofsky, S.T., et al. (2021). Mask, the
1094 Drosophila Ankyrin Repeat and KH Domain-Containing Protein, Affects Microtubule

1095 Stability. J. Cell Sci. 134 (20). doi: 10.1242/JCS.258512.
1096 Massey, J.H., Akiyama, N., Bien, T., Dreisewerd, K., Wittkopp, P.J., Yew, J.Y., et al. (2019).
1097 Pleiotropic Effects of Ebony and Tan on Pigmentation and Cuticular Hydrocarbon
1098 Composition in Drosophila Melanogaster. Front. Physiol. 10 (MAY): 518. doi:
1099 10.3389/FPHYS.2019.00518/BIBTEX.
1100 McGary, K.L., Park, T.J., Woods, J.O., Cha, H.J., Wallingford, J.B., and Marcotte, E.M. (2010).
1101 Systematic Discovery of Nonobvious Human Disease Models through Orthologous
1102 Phenotypes. Proc. Natl. Acad. Sci. U. S. A. 107 (14): 6544–49. doi:
1103 10.1073/pnas.0910200107.
1104 McKinnon, C., Snoo, M.L. De, Gondard, E., Neudorfer, C., Chau, H., Ngana, S.G., et al. (2020).
1105 Early-Onset Impairment of the Ubiquitin-Proteasome System in Dopaminergic Neurons
1106 Caused by α-Synuclein. Acta Neuropathol. Commun. 8 (1). doi: 10.1186/S40478-020-
1107 0894-0.
1108 Meiser, J., Weindl, D., and Hiller, K. (2013). Complexity of Dopamine Metabolism. Cell
1109 Commun. Signal. 11 (1). doi: 10.1186/1478-811X-11-34.
1110 Morin, X., Daneman, R., Zavortink, M., and Chia, W. (2001). A Protein Trap Strategy to Detect
1111 GFP-Tagged Proteins Expressed from Their Endogenous Loci in Drosophila. Proc. Natl.
1112 Acad. Sci. U. S. A. 98 (26): 15050. doi: 10.1073/PNAS.261408198.
1113 Mummery-Widmer, J.L., Yamazaki, M., Stoeger, T., Novatchkova, M., Bhalerao, S., Chen, D., et
1114 al. (2009). Genome-Wide Analysis of Notch Signalling in Drosophila by Transgenic RNAi.
1115 Nature 458 (7241): 987–92. doi: 10.1038/nature07936.
1116 Nakashima, A., Ohnuma, S., Kodani, Y., Kaneko, Y.S., Nagasaki, H., Nagatsu, T., et al. (2016).
1117 Inhibition of Deubiquitinating Activity of USP14 Decreases Tyrosine Hydroxylase
1118 Phosphorylated at Ser19 in PC12D Cells. Biochem. Biophys. Res. Commun. 472 (4): 598–
1119 602. doi: 10.1016/J.BBRC.2016.03.022.
1120 Ni, J.Q., Liu, L.P., Binari, R., Hardy, R., Shim, H.S., Cavallaro, A., et al. (2009). A Drosophila

1121 Resource of Transgenic RNAi Lines for Neurogenetics. Genetics 182 (4): 1089–1100. doi:
1122 10.1534/GENETICS.109.103630.
1123 Ni, J.Q., Markstein, M., Binari, R., Pfeiffer, B., Liu, L.P., Villalta, C., et al. (2007). Vector and
1124 Parameters for Targeted Transgenic RNA Interference in Drosophila Melanogaster. Nat.
1125 Methods 2008 51 5 (1): 49–51. doi: 10.1038/nmeth1146.
1126 Ni, J.Q., Zhou, R., Czech, B., Liu, L.P., Holderbaum, L., Yang-Zhou, D., et al. (2011). A
1127 Genome-Scale ShRNA Resource for Transgenic RNAi in Drosophila. Nat. Methods 8 (5):
1128 405–7. doi: 10.1038/NMETH.1592.
1129 Nicklas, W. m. do. J., Vyas, I., and Heikkila, R.E. (1985). Inhibition of NADH-Linked Oxidation in
1130 Brain Mitochondria by 1-Methyl-4-Phenyl-Pyridine, a Metabolite of the Neurotoxin, 1-
1131 Methyl-4-Phenyl-1,2,5,6-Tetrahydropyridine. Life Sci. 36 (26): 2503–8. doi: 10.1016/0024-
1132 3205(85)90146-8.
1133 Nutt, D.J., Lingford-Hughes, A., Erritzoe, D., and Stokes, P.R.A. (2015). The Dopamine Theory
1134 of Addiction: 40 Years of Highs and Lows. Nat. Rev. Neurosci. 16 (5): 305–12. doi:
1135 10.1038/NRN3939.
1136 Oh, H., and Irvine, K.D. (2010). Yorkie: The Final Destination of Hippo Signaling. Trends Cell
1137 Biol. 20 (7): 410. doi: 10.1016/J.TCB.2010.04.005.
1138 Pan, Y., Li, W., Deng, Z., Sun, Y., Ma, X., Liang, R., et al. (2022). Myc Suppresses Male-Male
1139 Courtship in Drosophila. EMBO J. 41 (7). doi: 10.15252/EMBJ.2021109905.
1140 Pan, Y., and Monje, M. (2020). Activity Shapes Neural Circuit Form and Function: A Historical
1141 Perspective. J. Neurosci. 40 (5): 944. doi: 10.1523/JNEUROSCI.0740-19.2019.
1142 Pendleton, R.G., Rasheed, A., Sardina, T., Tully, T., and Hillman, R. (2002). Effects of Tyrosine
1143 Hydroxylase Mutants on Locomotor Activity in Drosophila: A Study in Functional Genomics.
1144 Behav. Genet. 32 (2): 89–94. doi: 10.1023/A:1015279221600.
1145 Radwan, B., Liu, H., and Chaudhury, D. (2019). The Role of Dopamine in Mood Disorders and
1146 the Associated Changes in Circadian Rhythms and Sleep-Wake Cycle. Brain Res. 1713

1147 (June): 42–51. doi: 10.1016/J.BRAINRES.2018.11.031.
1148 Rezatabar, S., Karimian, A., Rameshknia, V., Parsian, H., Majidinia, M., Kopi, T.A., et al. (2019).
1149 RAS/MAPK Signaling Functions in Oxidative Stress, DNA Damage Response and Cancer
1150 Progression. J. Cell. Physiol. 234 (9): 14951–65. doi: 10.1002/JCP.28334.
1151 Richardt, A., Rybak, J., Störtkuhl, K.F., Meinertzhagen, I.A., and Hovemann, B.T. (2002). Ebony
1152 Protein in the Drosophila Nervous System: Optic Neuropile Expression in Glial Cells. J.
1153 Comp. Neurol. 452 (1): 93–102. doi: 10.1002/CNE.10360.
1154 Riemensperger, T., Isabel, G., Coulom, H., Neuser, K., Seugnet, L., Kume, K., et al. (2011).
1155 Behavioral Consequences of Dopamine Deficiency in the Drosophila Central Nervous
1156 System. Proc. Natl. Acad. Sci. U. S. A. 108 (2): 834–39. doi: 10.1073/PNAS.1010930108.
1157 Riemensperger, T., Issa, A.R., Pech, U., Coulom, H., Nguyễn, M.V., Cassar, M., et al. (2013). A
1158 Single Dopamine Pathway Underlies Progressive Locomotor Deficits in a Drosophila Model
1159 of Parkinson Disease. Cell Rep. 5 (4): 952–60. doi: 10.1016/J.CELREP.2013.10.032.
1160 Rohwedder, A., Wenz, N.L., Stehle, B., Huser, A., Yamagata, N., Zlatic, M., et al. (2016). Four
1161 Individually Identified Paired Dopamine Neurons Signal Reward in Larval Drosophila. Curr.
1162 Biol. 26 (5): 661–69. doi: 10.1016/J.CUB.2016.01.012.
1163 Sansores-Garcia, L., Atkins, M., Moya, I.M., Shahmoradgoli, M., Tao, C., Mills, G.B., et al.
1164 (2013). Mask Is Required for the Activity of the Hippo Pathway Effector Yki/YAP. Curr. Biol.
1165 23 (3): 229–35. doi: 10.1016/J.CUB.2012.12.033.
1166 Sekine, Y., Hatanaka, R., Watanabe, T., Sono, N., Iemura, S. ichiro, Natsume, T., et al. (2012).
1167 The Kelch Repeat Protein KLHDC10 Regulates Oxidative Stress-Induced ASK1 Activation
1168 by Suppressing PP5. Mol. Cell 48 (5): 692–704. doi: 10.1016/J.MOLCEL.2012.09.018.
1169 Sekine, Y., Takagahara, S., Hatanaka, R., Watanabe, T., Oguchi, H., Noguchi, T., et al. (2011).
1170 P38 MAPKs Regulate the Expression of Genes in the Dopamine Synthesis Pathway
1171 through Phosphorylation of NR4A Nuclear Receptors. J. Cell Sci. 124 (Pt 17): 3006–16.
1172 doi: 10.1242/JCS.085902.

1173 Sen, A., and Cox, R.T. (2016). Clueless Is a Conserved Ribonucleoprotein That Binds the
1174 Ribosome at the Mitochondrial Outer Membrane. Biol. Open 5 (2): 195–203. doi:
1175 10.1242/BIO.015313/-/DC1.
1176 Sen, A., Damm, V.T., and Cox, R.T. (2013). Drosophila Clueless Is Highly Expressed in Larval
1177 Neuroblasts, Affects Mitochondrial Localization and Suppresses Mitochondrial Oxidative
1178 Damage. PLoS One 8 (1). doi: 10.1371/JOURNAL.PONE.0054283.
1179 Sen, A., Kalvakuri, S., Bodmer, R., and Cox, R.T. (2015). Clueless, a Protein Required for
1180 Mitochondrial Function, Interacts with the PINK1-Parkin Complex in Drosophila. Dis.
1181 Model. Mech. 8 (6): 577–89. doi: 10.1242/DMM.019208.
1182 Shafer, O.T., and Keene, A.C. (2021). The Regulation of Drosophila Sleep. Curr. Biol. 31 (1):
1183 R38–49. doi: 10.1016/J.CUB.2020.10.082.
1184 Shimizu, J., Kasai, T., Yoshida, H., Huynh, A.M., Nakao-Azuma, Y., Shinomoto, M., et al.
1185 (2020). Novel Drosophila Model for Parkinsonism by Targeting Phosphoglycerate Kinase.
1186 Neurochem. Int. 139 (October). doi: 10.1016/J.NEUINT.2020.104816.
1187 Sidor, C., Borreguero-Munoz, N., Fletcher, G.C., Elbediwy, A., Guillermin, O., and Thompson,
1188 B.J. (2019). Mask Family Proteins ANKHD1 and ANKRD17 Regulate YAP Nuclear Import
1189 and Stability. Elife 8 (October). doi: 10.7554/ELIFE.48601.
1190 Sidor, C.M., Brain, R., and Thompson, B.J. (2013). Mask Proteins Are Cofactors of Yorkie/YAP
1191 in the Hippo Pathway. Curr. Biol. 23 (3): 223–28. doi: 10.1016/J.CUB.2012.11.061.
1192 Smith, R.K., Carroll, P.M., Allard, J.D., and Simon, M.A. (2002). MASK, a Large Ankyrin Repeat
1193 and KH Domain-Containing Protein Involved in Drosophila Receptor Tyrosine Kinase
1194 Signaling. Development 129 (1): 71–82. doi: 10.1242/DEV.129.1.71.
1195 Snel, B., Lehmann, G., Bork, P., and Huynen, M.A. (2000). STRING: A Web-Server to Retrieve
1196 and Display the Repeatedly Occurring Neighbourhood of a Gene. Nucleic Acids Res. 28
1197 (18): 3442. doi: 10.1093/NAR/28.18.3442.
1198 Spana, E.P., Abrams, A.B., Ellis, K.T., Klein, J.C., Ruderman, B.T., Shi, A.H., et al. (2020).

1199 Speck, First Identified in Drosophila Melanogaster in 1910, Is Encoded by the
1200 Arylalkalamine N-Acetyltransferase (AANAT1) Gene. G3 (Bethesda). 10 (9): 3387–98. doi:
1201 10.1534/G3.120.401470.
1202 Spanos, M., Gras-Najjar, J., Letchworth, J.M., Sanford, A.L., Toups, J.V., and Sombers, L.A.
1203 (2013). Quantitation of Hydrogen Peroxide Fluctuations and Their Modulation of Dopamine
1204 Dynamics in the Rat Dorsal Striatum Using Fast-Scan Cyclic Voltammetry. ACS Chem.
1205 Neurosci. 4 (5): 782–89. doi: 10.1021/CN4000499.
1206 Steiner, H., and Kitai, S.T. (2001). Unilateral Striatal Dopamine Depletion: Time-Dependent
1207 Effects on Cortical Function and Behavioural Correlates. Eur. J. Neurosci. 14 (8): 1390–
1208 1404. doi: 10.1046/J.0953-816X.2001.01756.X.
1209 Sugumaran, M., and Barek, H. (2016). Critical Analysis of the Melanogenic Pathway in Insects
1210 and Higher Animals. Int. J. Mol. Sci. 17 (10). doi: 10.3390/IJMS17101753.
1211 Sun, F., Zhou, J., Dai, B., Qian, T., Zeng, J., Li, X., et al. (2020). Next-Generation GRAB
1212 Sensors for Monitoring Dopaminergic Activity in Vivo. Nat. Methods 17 (11): 1156. doi:
1213 10.1038/S41592-020-00981-9.
1214 Szklarczyk, D., Gable, A.L., Nastou, K.C., Lyon, D., Kirsch, R., Pyysalo, S., et al. (2021). The
1215 STRING Database in 2021: Customizable Protein–Protein Networks, and Functional
1216 Characterization of User-Uploaded Gene/Measurement Sets. Nucleic Acids Res. 49 (D1):
1217 D605. doi: 10.1093/NAR/GKAA1074.
1218 Szklarczyk, D., Kirsch, R., Koutrouli, M., Nastou, K., Mehryary, F., Hachilif, R., et al. (2023). The
1219 STRING Database in 2023: Protein–Protein Association Networks and Functional
1220 Enrichment Analyses for Any Sequenced Genome of Interest. Nucleic Acids Res. 51 (D1):
1221 D638. doi: 10.1093/NAR/GKAC1000.
1222 Takahashi, A. (2013). Pigmentation and Behavior: Potential Association through Pleiotropic
1223 Genes in Drosophila. Genes Genet. Syst. 88 (3): 165–74. doi: 10.1266/GGS.88.165.
1224 Takáts, S., Pircs, K., Nagy, P., Varga, Á., Kárpáti, M., Hegedus, K., et al. (2014). Interaction of

1225 the HOPS Complex with Syntaxin 17 Mediates Autophagosome Clearance in Drosophila.
1226 Mol. Biol. Cell 25 (8): 1338–54. doi: 10.1091/MBC.E13-08-0449.
1227 Tank, A.W., Xu, L., Chen, X., Radcliffe, P., and Sterling, C.R. (2008). Post-Transcriptional
1228 Regulation of Tyrosine Hydroxylase Expression in Adrenal Medulla and Brain. Ann. N. Y.
1229 Acad. Sci. 1148: 238–48. doi: 10.1196/ANNALS.1410.054.
1230 Tekin, I., Roskoski, R., Carkaci-Salli, N., and Vrana, K.E. (2014). Complex Molecular Regulation
1231 of Tyrosine Hydroxylase. J. Neural Transm. 121 (12): 1451–81. doi: 10.1007/S00702-014-
1232 1238-7.
1233 Terhzaz, S., Cabrero, P., Chintapalli, V.R., Davies, S.A., and Dow, J.A.T. (2010). Mislocalization
1234 of Mitochondria and Compromised Renal Function and Oxidative Stress Resistance in
1235 Drosophila SesB Mutants. Physiol. Genomics 41 (1): 33–41. doi:
1236 10.1152/PHYSIOLGENOMICS.00147.2009.
1237 True, J.R., Edwards, K.A., Yamamoto, D., and Carroll, S.B. (1999). Drosophila Wing Melanin
1238 Patterns Form by Vein-Dependent Elaboration of Enzymatic Prepatterns. Curr. Biol. 9 (23):
1239 1382–91. doi: 10.1016/S0960-9822(00)80083-4.
1240 Valente, E.M., Abou-Sleiman, P.M., Caputo, V., Muqit, M.M.K., Harvey, K., Gispert, S., et al.
1241 (2004). Hereditary Early-Onset Parkinson's Disease Caused by Mutations in PINK1.
1242 Science (80-.). 304 (5674): 1158–60. doi: 10.1126/science.1096284.
1243 Vié, A., Cigna, M., Toci, R., and Birman, S. (1999). Differential Regulation of Drosophila
1244 Tyrosine Hydroxylase Isoforms by Dopamine Binding and CAMP-Dependent
1245 Phosphorylation. J. Biol. Chem. 274 (24): 16788–95. doi: 10.1074/JBC.274.24.16788.
1246 Vissers, J.H.A., Manning, S.A., Kulkarni, A., and Harvey, K.F. (2016). A Drosophila RNAi Library
1247 Modulates Hippo Pathway-Dependent Tissue Growth. Nat. Commun. 2016 71 7 (1): 1–6.
1248 doi: 10.1038/ncomms10368.
1249 Wang, J., Lou, H., Pedersen, C.J., Smith, A.D., and Perez, R.G. (2009). 14-3-3zeta Contributes
1250 to Tyrosine Hydroxylase Activity in MN9D Cells: Localization of Dopamine Regulatory

1251 Proteins to Mitochondria. J. Biol. Chem. 284 (21): 14011–19. doi:
1252 10.1074/JBC.M901310200.
1253 Wang, Z., Ferdousy, F., Lawal, H., Huang, Z., Daigle, J.G., Izevbaye, I., et al. (2011).
1254 Catecholamines up Integrates Dopamine Synthesis and Synaptic Trafficking. J.
1255 Neurochem. 119 (6): 1294–1305. doi: 10.1111/J.1471-4159.2011.07517.X.
1256 Wang, Z.H., Clark, C., and Geisbrecht, E.R. (2016). Drosophila Clueless Is Involved in Parkin-
1257 Dependent Mitophagy by Promoting VCP-Mediated Marf Degradation. Hum. Mol. Genet.
1258 25 (10): 1946–64. doi: 10.1093/HMG/DDW067.
1259 Wicker-Thomas, C., and Hamann, M. (2008). Interaction of Dopamine, Female Pheromones,
1260 Locomotion and Sex Behavior in Drosophila Melanogaster. J. Insect Physiol. 54 (10–11):
1261 1423–31. doi: 10.1016/J.JINSPHYS.2008.08.005.
1262 William Langston, J., Ballard, P., Tetrud, J.W., and Irwin, I. (1983). Chronic Parkinsonism in
1263 Humans Due to a Product of Meperidine-Analog Synthesis. Science 219 (4587): 979–80.
1264 doi: 10.1126/SCIENCE.6823561.
1265 Wittkopp, P.J., True, J.R., and Carroll, S.B. (2002). Reciprocal Functions of the Drosophila
1266 Yellow and Ebony Proteins in the Development and Evolution of Pigment Patterns.
1267 Development 129 (8): 1849–58. doi: 10.1242/DEV.129.8.1849.
1268 Wright, T.R.F., Bewley, G.C., and Sherald, A.F. (1976). The Genetics of Dopa Decarboxylase in
1269 Drosophila Melanogaster. II. Isolation and Characterization of Dopa-Decarboxylase-
1270 Deficient Mutants and Their Relationship to the Alpha-Methyl-Dopa-Hypersensitive
1271 Mutants. Genetics 84 (2): 287–310. doi: 10.1093/GENETICS/84.2.287.
1272 Xie, T., Ho, M.C.W., Liu, Q., Horiuchi, W., Lin, C.C., Task, D., et al. (2018). A Genetic Toolkit for
1273 Dissecting Dopamine Circuit Function in Drosophila. Cell Rep. 23 (2): 652–65. doi:
1274 10.1016/J.CELREP.2018.03.068.
1275 Xu, C., Luo, J., He, L., Montell, C., and Perrimon, N. (2017). Oxidative Stress Induces Stem Cell
1276 Proliferation via TRPA1/RyR-Mediated Ca2+ Signaling in the Drosophila Midgut. Elife 6

1277 (May). doi: 10.7554/ELIFE.22441.
1278 Yamamoto-Hino, M., Yoshida, H., Ichimiya, T., Sakamura, S., Maeda, M., Kimura, Y., et al.
1279 (2015). Phenotype-Based Clustering of Glycosylation-Related Genes by RNAi-Mediated
1280 Gene Silencing. Genes Cells 20 (6): 521–42. doi: 10.1111/GTC.12246.
1281 Yamamoto, S., Charng, W.-L., Rana, N.A., Kakuda, S., Jaiswal, M., Bayat, V., et al. (2012). A
1282 Mutation in EGF Repeat-8 of Notch Discriminates Between Serrate/Jagged and Delta
1283 Family Ligands. Science (80-.). 338 (6111): 1229–32. doi: 10.1126/science.1228745.
1284 Yamamoto, S., Jaiswal, M., Charng, W.-L., Gambin, T., Karaca, E., Mirzaa, G., et al. (2014). A
1285 Drosophila Genetic Resource of Mutants to Study Mechanisms Underlying Human Genetic
1286 Diseases. Cell 159 (1): 200–214. doi: 10.1016/j.cell.2014.09.002.
1287 Yamamoto, S., Kanca, O., Wangler, M.F., and Bellen, H.J. (2023). Integrating Non-Mammalian
1288 Model Organisms in the Diagnosis of Rare Genetic Diseases in Humans. Nat. Rev. Genet.
1289 In press.
1290 Yamamoto, S., and Seto, E.S. (2014). Dopamine Dynamics and Signaling in Drosophila: An
1291 Overview of Genes, Drugs and Behavioral Paradigms. Exp. Anim. 63 (2): 107–19. doi:
1292 10.1538/EXPANIM.63.107.
1293 Yang, H., Sibilla, C., Liu, R., Yun, J., Hay, B.A., Blackstone, C., et al. (2022). Clueless/CLUH
1294 Regulates Mitochondrial Fission by Promoting Recruitment of Drp1 to Mitochondria. Nat.
1295 Commun. 13 (1). doi: 10.1038/S41467-022-29071-4.
1296 Yoon, S., and Baik, J.H. (2013). Dopamine D2 Receptor-Mediated Epidermal Growth Factor
1297 Receptor Transactivation through a Disintegrin and Metalloprotease Regulates
1298 Dopaminergic Neuron Development via Extracellular Signal-Related Kinase Activation. J.
1299 Biol. Chem. 288 (40): 28435–46. doi: 10.1074/JBC.M113.461202.
1300 Zeitlinger, J., and Bohmann, D. (1999). Thorax Closure in Drosophila: Involvement of Fos and
1301 the JNK Pathway. Development 126 (17): 3947–56. doi: 10.1242/DEV.126.17.3947.
1302 Zhang, S., Wang, R., and Wang, G. (2019). Impact of Dopamine Oxidation on Dopaminergic

1303 Neurodegeneration. ACS Chem. Neurosci. 10 (2): 945–53. doi:
1304 10.1021/ACSCHEMNEURO.8B00454/ASSET/IMAGES/MEDIUM/CN-2018-
1305 004545_0005.GIF.
1306 Zhang, Y.Q., Friedman, D.B., Wang, Z., Woodruff, E., Pan, L., O'Donnell, J., et al. (2005).
1307 Protein Expression Profiling of the Drosophila Fragile X Mutant Brain Reveals Up-
1308 Regulation of Monoamine Synthesis. Mol. Cell. Proteomics 4 (3): 278–90. doi:
1309 10.1074/mcp.M400174-MCP200.
1310 Zhu, M., Li, X., Tian, X., and Wu, C. (2015). Mask Loss-of-Function Rescues Mitochondrial
1311 Impairment and Muscle Degeneration of Drosophila Pink1 and Parkin Mutants. Hum. Mol.
1312 Genet. 24 (11): 3272–85. doi: 10.1093/HMG/DDV081.
1313 Zhu, M., Zhang, S., Tian, X., and Wu, C. (2017). Mask Mitigates MAPT- and FUS-Induced
1314 Degeneration by Enhancing Autophagy through Lysosomal Acidification. Autophagy 13
1315 (11): 1924–38. doi: 10.1080/15548627.2017.1362524.
1316